Journal of Sound and Vibration 329 (2010) 3721–3743

Contents lists available at ScienceDirect

Journal of Sound and Vibration

journal homepage: www.elsevier.com/locate/jsvi

On the use of a uniformly valid analytical cascade response function for fan broadband noise predictions

H. Posson [a,*], S. Moreau [a], M. Roger [b]

[a] GAUS, Département de Génie Mécanique, Université de Sherbrooke, 2500 Bd. de l'université, Sherbrooke, QC, Canada J1H4X2
[b] Laboratoire de Mécanique des Fluides et Acoustique, École Centrale de Lyon, 36 Av. Guy de Colongue, 69131 Écully Cedex, France

ARTICLE INFO

Article history:
Received 6 August 2009
Received in revised form
3 March 2010
Accepted 4 March 2010
Handling Editor: P. Joseph
Available online 21 April 2010

ABSTRACT

The present paper extends an existing analytical model of the aeroacoustic response of a rectilinear cascade of flat-plate blades to three-dimensional incident vortical gusts, to the prediction of the noise generated by a three-dimensional annular blade-row. The extended formulation is meant to be implemented in a fan broadband noise prediction tool. The intended applications include the modern turbofan engines, for which analytical modelling is believed to be a good alternative to more expensive numerical techniques. The prediction noise model resorts to a strip theory approach based on a three-dimensional rectilinear cascade model. The latter is based on the Wiener–Hopf technique, and yields the pressure field in the blade passage and the unsteady blade loading. The analytical pressure solution is derived by making an extensive use of the residue theorem. The obtained unsteady blade loading distribution over the blades is then used as a dipole source distribution in an acoustic analogy applied in the annular rigid duct with uniform mean flow. The new achievements are then tested on three-dimensional annular-benchmark configurations and compared with three-dimensional lifting-surface models and three-dimensional Euler linearized codes available in the literature. The accuracy of the model is shown for high hub-to-tip ratio cases. When used as such in a true rectilinear-cascade configuration, it also reproduces the exact radiated field that can be derived directly. For low hub-to-tip ratio configurations, the model departs from three-dimensional computations, both regarding the blade loading and the acoustic radiation. A correction is proposed to account for the actual annular dispersion relation in the rectilinear-cascade response function. The results suggest that the proposed correction is necessary to get closer to the underlying physics of the annular-space wave equation, but that it is yet not sufficient to fully reproduce three-dimensional results.

1. Introduction

The long-term future of the aeroengine market is closely related to the expected sustained growth of air transport, which in turn is acceptable under the constraint of reduced exposure of populations around airports to both high noise levels and pollutant emissions. Therefore the acoustic signature is one of the main concerns, for current turbofan engines as well as for new propulsion systems under development. This established fact points out a critical need for practical

* Corresponding author. Tel.: +1 819 821 8000x62085; fax: +1 819 821 7163.
E-mail addresses: helene.posson@usherbrooke.ca, helene.posson@gmail.com (H. Posson), stephane.moreau@usherbrooke.ca (S. Moreau), michel.roger@ec-lyon.fr (M. Roger).

0022-460X/$ - see front matter © 2010 Elsevier Ltd. All rights reserved.
doi:10.1016/j.jsv.2010.03.009

Nomenclature

Latin characters

B_R number of blades
B_S number of vanes
c blade chord length in cascade reference frame (m)
$c_d = c/\cos\varphi$ blade chord length at constant radius (m)
c_0 speed of sound ($m\,s^{-1}$)
d chordwise non-overlap length (stagger distance) (m)
D kernel function in the Fourier transform of the potential jump $\Delta\phi$ across the blade of the rectilinear cascade
$E_{m,\mu}$ duct eigenfunction of the mode (m,μ)
$G_d(\mathbf{x}_d,t|\mathbf{x}_{d0},t_0)$ Green's function tailored to the annular duct with uniform mean flow, for a source in $\mathbf{x}_{d0}$ at t_0 and a receiver in $\mathbf{x}_d$ at time t
h inter-blade distance normal to the blades (m)
$H=R_H/R_T$ annular duct hub-to-tip ratio
$H_0^{(2)}(x)$ Hankel function of second kind of order 0
$k_0=\omega/c_0$ acoustic wavenumber (m^{-1})
$k^{\pm}_{x,m\mu}$ axial wavenumber of the duct mode (m,μ) $(k^{\pm}_{x,m\mu}=(-M_{x_d}k_0\mp\kappa_{m,\mu})/(\beta^2_{x_d}))$ (m^{-1})
$k^{\pm}_{x,m\mu,\mathrm{cd}}(r)$ axial wavenumber of the duct mode (m,μ) in the cascade reference frame before the rotation of sweep angle [1] $(k^{\pm}_{x,m\mu,\mathrm{cd}}=Q_{\check{\chi}\psi,11}k^{\pm}_{x,m\mu}-Q_{\check{\chi}\psi,12}m/r_0)$ (m^{-1})
$(k_{x_{c0}},k_{y_{c0}},k_{z_{c0}})$ Wavenumber of the incident gust in the cascade coordinate system (m^{-1})
$M_{xd}=U_{xd}/c_0$ axial Mach number
m azimuthal order of an acoustic duct mode
μ radial order of an acoustic duct mode
m_g azimuthal order of the incident gust
$\hat{p}^{\pm}(\mathbf{x}_d,\omega)$ acoustic pressure at point $\mathbf{x}_d$ upstream or downstream at angular frequency ω
p^s, p^p pressure on suction and pressure side of a blade, respectively (Pa)
$\mathcal{P}^{\pm}_{m,\mu}(\omega)$ amplitude of the duct mode (m,μ)
$\mathbf{Q}_{\check{\chi}\psi}$ transformation matrix from duct $\mathcal{R}_\mathrm{I}$ to cascade reference frame $\mathcal{R}_\mathrm{cd}$ [1]
$\mathbf{Q}_{\check{\chi}\psi\varphi}$ transformation matrix from duct $\mathcal{R}_\mathrm{I}$ to cascade reference frame $\mathcal{R}_c$ [1]
$\mathbf{Q_i}=\mathbf{Q}^{-1}_{\check{\chi}\psi\varphi}$ inverse transformation matrix from $\mathcal{R}_c$ to $\mathcal{R}_\mathrm{I}$
$\mathbf{q}$ $\mathbf{q}=\mathbf{Q}_{\check{\chi}\psi\varphi}(2,:)=(-\sin\check{\chi}\cos\psi,\cos\check{\chi}\cos\psi,-\sin\psi)$
r studied radius (m)
R_H duct hub radius (m)
$R_m=(R_T+R_H)/2$ duct mean radius (m)
R_T duct tip radius (m)
s distance between two adjacent leading-edges [m]
$\mathbf{U}$ mean flow vector in the reference frame $\mathcal{R}_\mathrm{I}$ ($m\,s^{-1}$)
$(U_c,0,W_c)$ Mean flow components in the cascade coordinate system ($m\,s^{-1}$)
U_{xd} axial mean flow velocity ($m\,s^{-1}$)
U_θ azimuthal mean flow velocity ($m\,s^{-1}$)
(x_c,y_c,z_c) Cartesian coordinates in the cascade reference frame $\mathcal{R}_c$ (origin O_c), z_c spanwise (m)
$(x_{\mathrm{cd}},y_{\mathrm{cd}},z_{\mathrm{cd}})$ Cartesian coordinates in the cascade reference frame $\mathcal{R}_\mathrm{cd}$ (origin O_cd) before rotation of the sweep angle, z_cd along the radius (m)
$(x_\mathrm{I},y_\mathrm{I},z_\mathrm{I})$ Cartesian coordinates in the duct reference frame rotating with the blade row $\mathcal{R}_\mathrm{I}$ (origin O_I) (m)
(x_d,y_d,z_d) Cartesian coordinates in the absolute duct reference $\mathcal{R}_d$ (origin O_d) (m)
(x_d,r_d,θ_d) cylindrical coordinates in the absolute duct reference $\mathcal{R}_d$ (origin O_d) (m)
$x_{\mathrm{LE,I}}$ axial coordinate of the leading edge (sweep) taken to be 0 in $r=R_H$ (m)
$y_{\mathrm{LE,I}}$ tangential coordinate of the leading edge (lean) taken to be 0 in $r=R_H$ (m)

Greek characters

$\beta=\sqrt{1-M^2}$ compressibility parameter relative to the chordwise mean velocity U_c in the cascade reference frame $\mathcal{R}_c$
β_{xd} compressibility parameter for axial mean flow
γ specific ratio of air ($\gamma=1.4$)
$\Gamma_{m,\mu}$ square of the norm of the duct eigenfunction $(r,\theta_d)\mapsto E_{m,\mu}e^{im\theta_d}$ (m^2)
$\kappa_{m,\mu}$ $\kappa^2_{m,\mu}=k_0^2-\beta^2_{xd}\chi^2_{m,\mu}$ (m^{-1})
ρ_0 mean fluid density [$kg\,m^{-3}$]
φ sweep angle after stagger and lean [1] (rad)
$\check{\varphi}$ sweep angle in the duct reference frame [1] (rad)
φ sweep angle after stagger [1] (rad)
ψ stator lean angle in the duct reference frame [1] (rad)
σ inter-blade phase angle $(\sigma=k_{x_{c0}}d+k_{y_{c0}}h=2\pi m_g/B_\mathrm{I})$
$\check{\chi}$ stagger angle in the duct reference frame of the cascade [1] (rad)
$\chi=\arctan d/h$ rectilinear-cascade stagger angle (rad)
$\chi_{m,\mu}$ eigenvalue of the mode (m,μ) (m^{-1})
Ω_I cascade angular speed ($rad\,s^{-1}$)
ω_{ex} incident angular frequency ($rad\,s^{-1}$)
ω angular frequency ($rad\,s^{-1}$)
$\omega_g=\omega_{\mathrm{ex}}-k_{z_{c0}}W$ modified angular frequency ($rad\,s^{-1}$)

Subscript

I R (relative to the rotor) or S (relative to the stator)

Superscript

* conjugate of the complex

prediction schemes that can be used at the early design stage by engine manufacturers, and for a better understanding of the involved source and flow physics. Modern turbofan engines have larger diameters and higher bypass ratios for improved aircraft performance at lower nominal rotation speed, when compared to previous technologies. In the continuation of the improvements achieved in the past decades the reduction of jet noise related to lower exhaust velocities has made rotating blade noise dominant in the engine signature, especially in cut-back and approach conditions. Furthermore the relative contribution of the broadband noise sources turned out to be more significant because a considerable effort has been made towards the reduction of tonal noise, ensured by proper blade and vane counts, and suited blade design with lower rotational speeds and larger chords (e.g. NASA studies [2–8], Whittle laboratory results [9] or RESOUND European research project with a design of a fan with a reduced tip speed for tonal noise reduction [10]). As a result, apart from additional means such as passive attenuation of sound by liners, broadband noise reduction at the source remains a topic of major interest for the industry and for the research community in general. The continuous process of turbofan engine noise control in the past has shown that first steps are often very effective, but that further reductions become harder and harder. More accurate prediction schemes are now needed, able to reproduce the relative and absolute effects of the geometrical parameters of a fan, such as blade twist, sweep and lean in three-dimensional configurations.

Broadband noise mainly results from vortex dynamics in the presence of solid surfaces. This includes typically fan rotor noise due to ingestion of turbulence, stator noise due to the impingement of rotor wakes on outlet guide vanes, interaction of boundary layer growing on nacelle with tip blade, and trailing-edge noise due to boundary-layer turbulence scattering. The present work is fundamentally addressing the first two, as just examples of the general mechanism of turbulence-interaction noise. Now predictions dedicated to turbulence-interaction noise for aeronautical needs must be able to cover an extended frequency range, typically between 50 Hz and 8 kHz according to EPNL standards. This is a considerable task not only because of Reynolds and Mach numbers encountered in these complicated geometries, but also because the Helmholtz numbers k_0R_T and k_0c based on either the fan tip radius R_T or the blade chord c range up to typically 100 and 30, respectively. Computational resources capturing so different scales are simply not available or highly time-consuming, at least in a short-term for industrial purposes. This motivated the derivation of an analytical model for the sound produced by the impingement of a vortical gust on an annular blade row.

The analytical approach is preferred in this paper as a reasonable alternative, essentially because fast-running analytical models are more suited to the parametric studies required for the preliminary design of a fan. However, the necessary simplifications made to get closed-form solutions may result in some inaccuracy in the predictions, which therefore must be validated on dedicated test cases. Properly addressing the broadband noise problem would imply prediction schemes including both the effect of the mean swirl upstream or downstream of a blade row, and the main features of an actual annular three-dimensional blade geometry. Up to that point the simplifications must preserve blade twist, sweep and lean as the main parameters, but the true geometry is definitely not tractable. As an expectedly reliable compromise, an annular blade row can be described by a limited number of strips cut at different radii, in such a way that in each strip the geometry and the relative flow features can be considered constant in the radial direction. Each strip is unwrapped and defines an equivalent linear cascade with an infinite number of blades to ensure the periodicity. A blade in a strip is assimilated to a flat plate with zero thickness and camber, and the local relative mean flow over the blade is assumed uniform and parallel to the chord line. This view extends the slightly loaded airfoil assumptions of linearized unsteady aerodynamics to cascades. As pointed out by Evers and Peake [11], it is reliable for broadband noise evaluations based on a statistical analysis, whereas the real shape of the blades would have an important effect on the interferences producing the tonal noise from periodic wake interactions. Finally the effect of a swirling mean flow on the sound radiation, on the possible coupling with inertial, hydrodynamic modes of oscillation and on the dynamics of the wakes is not considered here, but the model is developed in such a way that it can be extended to account for it in the future. Thus, Green's function tailored to the duct with swirling mean flow could be developed following the method of Heaton and Peake [12] and integrated to the model.

The crucial step in the method is the determination of the response of a linear cascade to incident vortical disturbances, which practically are the Fourier components of a turbulent velocity field. Different formulations and techniques have been proposed in the literature. A first class of methods that can be referred to as semi-numerical or semi-analytical has been mostly developed in the seventies, by Kaji and Okazaki [13,14] using a singularity method based on the acceleration, Whitehead [15,16] and Smith [17] using lifting-surface methods, Goldstein [18, Chapter 5] accounting for three-dimensional gusts and duct walls in a rectilinear configuration. All these methods require some numerical solving of an integral equation whereas closed-form expressions would be preferable for the sake of multiple calls in a statistical prediction scheme. Such expressions may be provided by models based on the Wiener–Hopf technique. So different solutions of the generic cascade response problem have been proposed in the past by Mani and Horvay [19], Koch [20], Peake [21,22], Peake and Kerschen [23], Majumdar and Peake [24]. The basis for the present derivations is Glegg's model [25], which is easily adapted to infer the cascade response for three-dimensional gusts and swept blades. This model has been recently extended by Posson and Roger [26] to provide closed-form expressions for the acoustic field inside the inter-blade channels, as well as for the pressure jump over the blades in subsonic flows. It must be noted that apart from approaches resorting to a rectilinear cascade, semi-numerical methods for a ducted three-dimensional annular cascade have also been developed by Namba [27], Kodama and Namba [28] and Schulten [29,30]. These methods have not been retained for the intended applications to realistic blade rows because they assume a zero stagger stator. Either related or not to cascade-response issues, a great deal of effort has been made over the last 40 years to predict the broadband noise

due to turbulence ingestion and wake interactions in rotating blade technology. Former models, notably introduced by Mani [31], Homicz and Georges [32], Amiet [33,34], Roger and Moreau [35] and Moreau and Roger [36] dealt with the interaction of an incident turbulence with an isolated airfoil. They were mostly dedicated to propellers or open rotors, the blade number of which is smaller than 10. In that case an isolated-airfoil response function is reliable. Yet current turbofan engines involve ducted rotors and stators with a high number of blades and vanes, for which in-duct propagation and cascade effects must be included in the prediction methods as two crucial points. Glegg [37], De Gouville [38], Joseph and Parry [39] developed broadband noise models for ducted fans using Green's function tailored to the duct and the unsteady blade loading as acoustic sources, in the usual sense of the acoustic analogy. Nevertheless, these investigations were based on isolated-airfoil response functions and the predictions may be abusive for blade rows with significant overlap between adjacent blades. Ventres et al. [40] were the first ones to propose a fan broadband noise model for inlet and wake turbulence considering both the duct and the cascade effects. An in-duct formulation of the acoustic analogy was again applied, using the unsteady blade loading as input data, but resorting to a two-dimensional cascade response function. The radial variation of the turbulence was indirectly taken into account by means of a strip theory. More recently, Nallasamy and Envia [41] improved the model and coupled it to a Reynolds-averaged Navier–Stokes computation to get the turbulence input data needed for the acoustic calculation. The application included both wake and background turbulence fields, and showed a satisfactory agreement with measurements. Another possible approach is to include the spanwise variations of the turbulence in the analysis with a three-dimensional rectilinear cascade model: the gust is three-dimensional but the cascade is still rectilinear. This refinement can be important when studying the rotor-stator interaction as shown by Ravindranath and Lakshminarayana [42] and Ganz et al. [43], or the ingestion of atmospheric turbulence by a rotor, e.g. Hanson [44]. Glegg and Walker [45], Hanson and Horan [46,1] and Evers and Peake [11] extended this type of method, successively including sweep and blade geometry effects. The predictions were found to be in a rather good agreement with experimental results, despite the *a priori* restrictive assumption of a rectilinear cascade [46].

The present paper is aimed at predicting the noise generated by an annular blade row in a turbulent inflow, accounting for cascade effects and the main three-dimensional geometrical and flow features, and resorting to an analytical cascade response function. The approach is based on a strip theory and on an extension [26] of Glegg's analytical solution [25]. The unsteady blade loading is calculated on a strip using closed-form expressions for the three-dimensional rectilinear-cascade response. It is then used as a dipole source distribution in the usual sense of the acoustic analogy. The wave equation for the guided sound field is solved using Green's function of an annular rigid duct with uniform mean flow. This strategy is motivated by the future implementation in an integrated turbulence-interaction noise prediction scheme. On the one hand, it must be distinguished from similar approaches in annular duct such as those of Ventres et al. [40] or Nallasamy and Envia [41], by the fact that the unsteady blade loading response of the cascade is three-dimensional: it accounts for spanwise wave-numbers, i.e. spanwise variations of the incident gust around the reference radius of a strip. On the other hand, it differs from the models of Glegg and Walker [45], Hanson and Horan [46,1] and Evers and Peake [11] by a different use of the cascade response. Here the unsteady loading is a direct source term in an acoustic analogy and radiates in an annular duct, whereas in other models the radiated field is computed directly in an equivalent rectilinear configuration without the explicit form of the pressure jump. The principle of the approach and the analytical formulation are first detailed in Section 2. A correction of the unsteady blade loading formulation in rectilinear cascade is proposed to better account for some of the three-dimensional effects. The strip-theory model is compared in Section 3 to fully three-dimensional computations for annuli of high and low hub-to-tip ratios, in the case of a zero stagger angle and of a swirl-free mean flow, as proposed by Hanson for the category 4 of the Third Computational Aeroacoustic benchmark [47]. Both the initial and corrected versions of the model are considered, showing the effectiveness of the correction. Finally the model is used to predict the wake-interaction broadband noise of the 22-in source diagnostic test (SDT) fan rig of the NASA Glenn Research Center [48–51] in Section 4.

2. Theoretical model

The key feature of the present work is the use of an explicit, analytical formulation for the unsteady response of a rectilinear cascade to an incoming vortical gust [26], extending Glegg's original analytical solution [25]. The extended formulation of the model provides closed-form expressions for the acoustic field in the inter-blade channels and the unsteady blade loading on a blade [26]. The paper is addressing the ability of the analytical solution to predict the broadband noise in a realistic three-dimensional annular cascade configuration with a reasonable accuracy, expecting faster computations from the rectilinear-cascade closed-form solution. Indeed the computational time is a major industrial constraint.

Two-dimensional test cases previously confirmed that the present rectilinear cascade response function agrees very well with numerical simulations in a thin annular duct for which the blade geometry and flow features do not vary significantly in the radial direction [26]. This suggests that the model can also be applied in a full three-dimensional annulus configuration, resorting to a strip-theory approach, as long as the quantity of interest is the induced unsteady lift used as a source term. However, complete geometrical parameters such as the blade surface curvature and the lack of

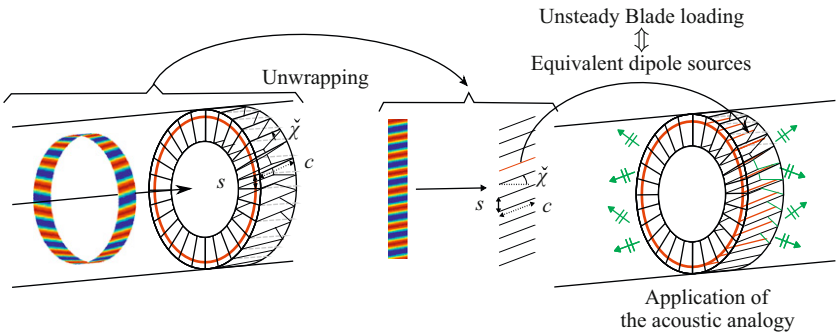

Fig. 1. Sketch of the principle of the method: split of the annular duct in strips, unwrapping of each strip in a rectilinear cascade and definition of the associated geometry and gust, computation of the unsteady blade-loading, injection of this pressure jump as equivalent dipole source on blades, computation of the radiated field.

parallelism between adjacent blades cannot be fully accounted for, even when splitting a blade into radial segments. It is therefore crucial to assess the effects and/or to propose suited corrections.

The way the three-dimensionality is indirectly simulated is illustrated in Fig. 1 and can be stated as follows. In any cylindrical cut, the helical gust that would be considered as the incident disturbance in cylindrical coordinates becomes an equivalent oblique gust. A finite radial extent is considered on each side of the cut, defining a strip over which the mean-flow parameters and the geometry are assumed constant in the radial direction. The three-dimensionality is preserved by means of the radial wavenumber associated with the obliqueness of the incident gust, whereas the local unsteady lift on the blades is assimilated to the one of a rectilinear cascade having the same parameters as the cut in the real blade row. This means that typically the effect of the non-parallelism is ignored in the response, which is strictly valid in the limit of an arbitrary large number of blades (or vanes).

In principle, due to the additional effect of the local curvature discarded by virtue of the flat-plate assumption, the unsteady lift distribution determined this way suffers from artificial jumps of phase and amplitude between adjacent strips, which would be prejudicial to a proper description of the acoustic sources for tonal noise prediction, essentially for noncompact blades. However, the jumps are not expected to be a serious drawback within the scope of a statistical analysis dedicated to broadband noise. Keeping this in mind, the unsteady lift becomes an equivalent dipole source in the acoustic analogy and its distribution over a blade will provide the acoustic modes of propagation in the duct, as discussed in the subsequent sections. Such a procedure at least includes the major effects caused by the variations of blade twist and radial solidity, which are expected to be the dominant three-dimensional effects.

2.1. Initial analytical formulation

The acoustic pressure produced by a blade row in an annular duct with axial uniform mean flow is expressed according to the acoustic analogy as function of the unsteady force per unit area $\mathbf{f}$ on the blades and Green's function tailored to the annular duct in uniform axial mean flow G_d. The latter $G_d(\mathbf{x}_d,t|\mathbf{x}_{d\,0},t_0)$ is expressed (see Goldstein [18, Chapter 4] for circular duct or Ventres et al. [40] for annular duct) in the time domain for a point and time impulse source $(\mathbf{x}_{d0},t_0)=(x_{d0},r_0,\theta_{d0},t_0)$ and a point and time of reception $(\mathbf{x}_d,t)=(x_d,r,\theta_d,t)$ by

$$G_d(\mathbf{x}_d,t|\mathbf{x}_{d0},t_0)=\frac{\mathrm{i}}{4\pi}\sum_{m=-\infty}^{+\infty}\sum_{\mu=0}^{+\infty}\frac{E_{m\mu}(r)E_{m\mu}(r_0)\mathrm{e}^{\mathrm{i}m(\theta_d-\theta_{d0})}}{\Gamma_{m\mu}}\int_{-\infty}^{\infty}\frac{\mathrm{e}^{\mathrm{i}k^{\pm}_{x,m\mu}(x_d-x_{d0})-\mathrm{i}\omega(t-t_0)}}{\kappa_{m\mu}}\,\mathrm{d}\omega. \tag{1}$$

The formulation is detailed here for a rotor under the impingement of inflow turbulence, but similar developments would follow for outlet guide vanes swept by turbulent rotor wakes. Only the dipole-like sources are considered and the quadrupole noise is neglected [18]. Since the viscous forces are neglected and the blades are assumed as flat plates, the net force $\mathbf{f}\,(\mathbf{x}_{d\,0},t_0)\,\mathrm{d}S$ across the blade j of surface S_j reduces to

$$[p^s(\mathbf{x}_{d0},t_0)-p^p(\mathbf{x}_{d0},t_0)]\,\mathrm{d}S_j\mathbf{n}_j=-\Delta P(\mathbf{x}_{d0},t_0)\,\mathrm{d}S_j\mathbf{n}_j$$

and the acoustic pressure reads

$$p^{\pm}(\mathbf{x}_d,t)=-\int_{-T}^{T}\int\int_{\cup_j S_j(t_0)}\frac{\partial G_d(\mathbf{x}_d,t|\mathbf{x}_{d0},t_0)}{\partial n}\Delta P(\mathbf{x}_{d0},t_0)\mathbf{n}_j\,\mathrm{d}S_j(\mathbf{x}_{d0})\,\mathrm{d}t_0. \tag{2}$$

After standard manipulations and changing from the reference frame $\mathcal{R}_d$ to a frame $\mathcal{R}_1$ rotating with the blade row, a different form follows as

$$\hat{p}^{\pm}(\mathbf{x}_d,\omega)=\sum_{m\in\mathbb{Z}}\sum_{\mu\in\mathbb{N}}\mathcal{P}^{\pm}_{m,\mu}(\omega)E_{m,\mu}(r)\mathrm{e}^{\mathrm{i}k^{\pm}_{x,m\mu}x_d+\mathrm{i}m\theta_d}, \tag{3}$$

where $E_{m,\mu}$ is the radial eigenfunction of the duct mode of orders (m,μ) and $\mathcal{P}^{\pm}_{m,\mu}(\omega)$ is its amplitude and is equal to

$$\mathcal{P}^{\pm}_{m,\mu}(\omega)=\frac{1}{2\mathrm{i}\kappa_{m,\mu}\Gamma_{m,\mu}}\int_{R_H}^{R_T}\int_0^{c_d(r_0)}\left[q_3\frac{\mathrm{d}}{\mathrm{d}r_0}+\mathrm{i}\left(q_2\frac{m}{r_0}-q_1k^{\pm}_{x,m\mu}\right)\right]E^*_{m,\mu}(r_0)\mathrm{e}^{-\mathrm{i}k^{\pm}_{x,m\mu,\mathrm{cd}}x_{\mathrm{cd}}}\times\sum_{j=0}^{B-1}\Delta\hat{P}_{\mathrm{cd},j}(x_{\mathrm{cd}},r_0,\omega-m\Omega_R)\mathrm{e}^{\mathrm{i}j2\pi m/B}\,\mathrm{d}x_{\mathrm{cd}}\mathrm{e}^{\mathrm{i}((m/r_0)y_{\mathrm{LE,I}}(r_0)-k^{\pm}_{x,m\mu}x_{\mathrm{LE,I}}(r_0))}\mathrm{d}r(\mathbf{x}_{\mathrm{I}0}). \tag{4}$$

$\Delta\hat{P}_{\mathrm{cd},j}(x_{\mathrm{cd}},r_0,\omega_{\mathrm{ex}})$ is the pressure jump at the radius r_0, on the blade j, for a chordwise position x_{cd} in the cascade reference frame $\mathcal{R}_{\mathrm{cd}}$ at the angular frequency of the incident excitation ω_{ex}. In the expression above, ω_{ex} is set equal to $\omega-m\Omega_R$. Indeed, due to its rotation at angular velocity Ω_R, the blade row induces a frequency scattering in addition to the modal scattering. The contribution of the azimuthal duct mode m to the acoustic pressure produced at the angular frequency ω is generated by the interaction of incident gusts at angular frequencies $\omega_{\mathrm{ex}}=\omega-m\Omega_R$. On the contrary, there is no frequency scattering in a stator as it is fixed with respect to the observer.

From Eq. (4), the pressure jump must be provided everywhere on the blade, that is to say, for each radius r_0, at every chordwise position x_{cd} along a line of constant radius $(\Delta\hat{P}_{\mathrm{cd},j}(x_{\mathrm{cd}},r_0,\omega_{\mathrm{ex}}))$. Yet, the rectilinear cascade model provides the unsteady blade loading $\Delta\hat{P}_{c,j}(x_c,\omega_{\mathrm{ex}}|r_0)$ along the chordwise distance x_c in the cascade reference frame $\mathcal{R}_c$ after rotation of the sweep angle, where r_0 is a mere parameter defining the cascade geometry, the excitation and the mean flow. These two expressions are linked by the relation:

$$\Delta\hat{P}_{\mathrm{cd},j}(x_{\mathrm{cd}},r_0,\omega_{\mathrm{ex}})\approx\Delta\hat{P}_{c,j}(x_{\mathrm{cd}}\cos\varphi,\omega_{\mathrm{ex}}|r_0)\mathrm{e}^{\mathrm{i}k_{z_{c0}}\sin\varphi x_{\mathrm{cd}}}, \tag{5a}$$

from inspection of the sketch in Fig. 2(b) if the blade row geometry and the incident excitation properties are assumed to be unchanged over a radial length $c_d\sin2\varphi$. In addition, the unsteady blade-loading on the blade j can be deduced from that on the blade 0 by a shift in phase of the j-times inter-blade phase angle σ:

$$\Delta\hat{P}_{c,j}(x_c,\omega_{\mathrm{ex}}|r_0)=\Delta\hat{P}_{c,0}(x_c,\omega_{\mathrm{ex}}|r_0)\mathrm{e}^{\mathrm{i}j\sigma}, \tag{5b}$$

since the blades encounter the same gust. These remarks lead to the final expression for the duct mode amplitude as

$$\mathcal{P}^{\pm}_{m,\mu}(\omega)=\frac{1}{2\mathrm{i}\kappa_{m,\mu}\Gamma_{m,\mu}}\int_{R_H}^{R_T}\left[q_3\frac{\mathrm{d}}{\mathrm{d}r_0}+\mathrm{i}\left(q_2\frac{m}{r_0}-q_1k^{\pm}_{x,m\mu}\right)\right]\times E^*_{m,\mu}(r_0)\sum_{j=0}^{B-1}\mathrm{e}^{\mathrm{i}j(\sigma+2\pi m/B)}IdP_{c,m,\mu}(r,\omega,\sigma,k_{z_{c0}})\mathrm{e}^{\mathrm{i}((m/r_0)y_{\mathrm{LE,I}}(r_0)-k^{\pm}_{x,m\mu}x_{\mathrm{LE,I}}(r_0))}\,\mathrm{d}r(\mathbf{x}_{\mathrm{I}0}), \tag{6a}$$

with

$$IdP_{c,m,\mu}(r,\omega,\sigma,k_{z_{c0}})=\int_0^c\Delta\hat{P}_{c,0}(x_c,\omega-m\Omega_R|r_0)\mathrm{e}^{\mathrm{i}\frac{(k_{z_{c0}}\sin\varphi-k^{\pm}_{x,m\mu,\mathrm{cd}})}{\cos\varphi}x_c}\frac{\mathrm{d}x_c}{\cos\varphi}. \tag{6b}$$

The chordwise integral $IdP_{c,m,\mu}$ can be calculated analytically at each radius from the rectilinear cascade model, whereas the radial integration is computed numerically, r being a parameter.

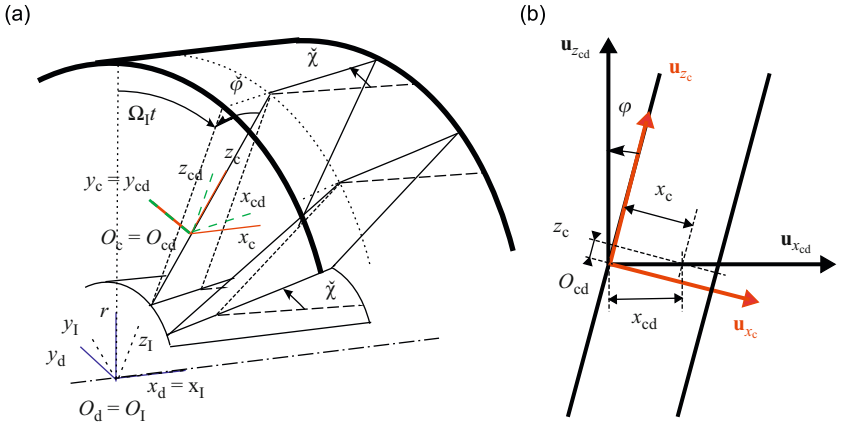

Fig. 2. (a) Sketch of the different reference frames used in the present model. The direct reference frames are $\mathcal{R}_d$ $(O_d,(x_d,y_d,z_d))$, a fixed reference frame linked to the duct, $\mathcal{R}_{\mathrm{I}}$ $(O_{\mathrm{I}},(x_{\mathrm{I}},y_{\mathrm{I}},z_{\mathrm{I}}))$ a relative reference frame linked to the annular blade row rotating at the angular velocity Ω_{I}, $\mathcal{R}_{\mathrm{cd}}$ $(O_{\mathrm{cd}},(x_{\mathrm{cd}},y_{\mathrm{cd}},z_{\mathrm{cd}}))$ and $\mathcal{R}_c(O_c,(x_c,y_c,z_c))$ two reference frames linked to the rectilinear cascade at a particular radius r, respectively, before and after rotation of the sweep angle φ. The sketch is plotted for a zero lean angle ψ; (b) geometrical parameters exhibited in the method to integrate the pressure jump along the whole blade: pressure jump in (x_{cd},r) is obtained by computed the pressure jump in x_c (in the reference frame $\mathcal{R}_c$) for the cascade geometry at the radius r and by taking the phase shift $\Delta z_c=x_{\mathrm{cd}}\sin\varphi$ into account.

2.2. Main issues of the approach

Applying a rectilinear-cascade response function within the scope of a strip theory may be somewhat questionable, regarding specific features of a three-dimensional cascade, such as the aforementioned non-parallelism of the blades, the modal scattering on radial orders, the spanwise non-uniformity of incident disturbances, and cut-off property issues. Attention must be paid to the possibly associated loss of accuracy in the predictions.

First, neither the strip theory nor the cascade model can cope with the expected modal scattering which occurs as an incident gust impinges on an annular cascade of realistic geometry. Indeed in the rectilinear unwrapped configuration with no sweep, only scattered modes with the same spanwise (radial) order as the incident mode can be generated, because the gusts are defined in a Cartesian reference frame for which the blade is aligned with a line of constant coordinate. In other words the spanwise wavenumber can be factored out, which is equivalent to repeat the trace of the incident gust on the leading edge into the scattered modes. In the same way incident helical gusts defined in cylindrical coordinates would be scattered as modes with the same radial trace by purely radial, untwisted blades in an annular cascade without walls. The radial modal scattering occurs in practice because of the mismatch between the geodesic lines of a blade surface and the lines of constant coordinates in the duct. This issue affects the accuracy of the unsteady blade loading as predicted by a rectilinear cascade model. Yet the strip-theory approach will generate more accurate relative contributions of all propagating modes in the annular duct thanks to the strip-by-strip account of the blade-twist and solidity radial variations, compared to a single strip approach. This is not considered for instance in the exact rectilinear formulation developed by Glegg [52] based on a single strip. Rectilinear formulations applied to several strips such as Hanson's model [1,46] try to address the previous limitation but are only approximate as they sum the contributions of each strip to the acoustic power in a statistical way. In the present approach the radiated field at any location within the duct results from the contributions of any radius according to the annular-duct formulation whereas it only results from the strip of the same radius in the aforementioned formulation.

Furthermore, the strip theory does not account for the non-parallelism of adjacent blades nor the presence of the duct walls in the evaluation of the unsteady blade loading. In particular, resonance effects expected between adjacent parallel blades excited by phased incoming disturbances should be much weaker between blades making a finite angle with each other. The annular-duct walls also induce modifications of the unsteady blade loading, differently from what the effects of parallel walls in a rectilinear cascade would be. Nevertheless the correct location of the sources on non-parallel blades and the presence of the walls are accounted for automatically when computing the in-duct propagation using the tailored Green's function.

Besides the response-function issues, the experimental studies of Raj and Lakshminarayana and Ravindranath and Lakshminarayana on the turbulence in rotor wakes [42,53], of Ganz on the variation of the turbulence intensity near the duct walls [43] and of Hanson on the ingestion of atmospheric turbulence by a rotor [44] show evidence of the strong spanwise variation of the turbulence upstream of the rotor blades or the outlet guide vanes of a turbofan. The excitation on the blade rows in a fan is then fully three-dimensional. Hence both the geometry of the blade row and the incident disturbances vary radially. A proper account for the spanwise non-uniformity of incident disturbances is then needed.

Finally another issue has been pointed out by Elhadidi and Atassi [54] about the cut-on frequencies predicted by strip-theory models. Indeed, a rectilinear-cascade model predicts scattered modes at cut-on frequencies which are functions of the geometry of the cascade, and of the spanwise mode order of the excitation. When the model is applied to a three-dimensional configuration, the cut-off or cut-on properties vary from one strip to another and again do not match what the response of an annular blade row would be. For instance cut-on conditions may be encountered at the tip and cut-off conditions at the hub. It is then relevant to check whether the predicted distribution of the acoustic energy over the modes is consistent or not, by comparing the model with a full three-dimensional computation. This will be done in Section 3. Finally, one can wonder whether the aforementioned shortcomings can be balanced by ad hoc corrections. A first attempt at such corrections is presented in the next section.

2.3. Corrected cascade-response model for a strip-theory application

A correction is proposed here to include some three-dimensional features in the rectilinear-cascade model presently applied to a strip, to yield a more realistic description of the unsteady blade loading. The previously derived expression of the unsteady blade loading has been presented in [26] from Glegg's original formulation [25]. Only the new aspects are detailed here. The potential disturbance ϕ in response to an incident vortical gust must make the total normal velocity zero on the blades, and ensure the Kutta condition of zero pressure jumps at the trailing edges and in the wakes. The potential must also be continuous upstream of the blades and is a solution of the convected wave equation:

$$\frac{1}{c_0^2}\frac{\mathrm{D}^2}{\mathrm{D}t^2}\phi-\nabla^2\phi=0. \tag{7}$$

Since it is discontinuous across the blades and wakes, generalized derivatives (operators with a prime) may be introduced for well-posed definition and integration [25]. This leads to the equation:

$$\acute{\Box}\,\phi=\frac{1}{c_0^2}\frac{\mathrm{D}^2\phi}{\mathrm{D}t^2}-\acute{\nabla}^2\phi=-\frac{\partial}{\partial y_c}\sum_{n\in\mathbb{Z}}\Delta\phi_n(x_c,z_c,t)\delta(y_c-nh), \tag{8}$$

where $\Delta\phi_n$ is the discontinuity of velocity potential across the blade numbered n. Dealing with a rectilinear cascade, the model is initially based on an equation written in Cartesian coordinates:

$$\acute{\Box} = \frac{1}{c_0^2}\left(\frac{\partial}{\partial t} + U_c\frac{\partial}{\partial x_c} + W_c\frac{\partial}{\partial z_c}\right)^2 - \frac{\partial^2}{\partial x_c^2} - \frac{\partial^2}{\partial y_c^2} - \frac{\partial^2}{\partial z_c^2}, \tag{9}$$

whereas the true annular configuration of the strip of interest should be described in cylindrical coordinates for which the operator reads

$$\acute{\Box} = \frac{1}{c_0^2}\left(\frac{\partial}{\partial t} + U_{xd}\frac{\partial}{\partial x_d} + U_\theta(r)\frac{\partial}{r\partial\theta}\right)^2 - \frac{\partial^2}{\partial x_d^2} - \frac{\partial^2}{r^2\partial\theta^2} - \frac{\partial^2}{\partial r^2} - \frac{\partial}{r\partial r}. \tag{10}$$

Furthermore monochromatic fluctuations are considered, so that the wave operator reduces to Helmholtz operator. In the annular case it is applied to a harmonic gust of the form $\Phi(x_c,y_c,z_c,t) = e^{im\theta_d + ik_{z_{d0}}r - ik_{x_d}x_d - i\omega_{ex}t}$ of associated equivalent Cartesian coordinate position ${}^t(x_d,y_d = -r\theta_d,z_d) = \mathbf{Q}_i^t(x_c,y_c,z_c)$ and wavenumber $\mathbf{K}_I = (-k_{x_d},-m/r,k_{z_{d0}})$ in the duct reference frame $\mathcal{R}_I$. This leads to the expression:

$$\acute{\Box}\,\Phi(x_c,y_c,z_c,t) = \left[-\left(\omega_{ex} + k_{x_d}U_{xd} - \frac{m}{r}U_\theta\right)^2/c_0^2 + k_{x_d}^2 + \left(\frac{m}{r}\right)^2 + k_{z_{d0}}^2 - i\frac{k_{z_{d0}}}{r}\right]\Phi(x_c,y_c,z_c,t). \tag{11}$$

The corresponding harmonic gust and wavenumber in the cascade reference frame $\mathcal{R}_c$ are $\Phi(x_c,y_c,z_c,t) = e^{-ik_{y_c}y_c + ik_{z_{c0}}z_c - ik_{x_c}x_c - i\omega_{ex}t}$ and $\mathbf{K}_c = (-k_{x_c},-k_{y_c},k_{z_{c0}}) = \mathbf{Q}_{\tilde{\chi}\psi\varphi}\mathbf{K}_I$ with the property that

$$\|\mathbf{K}_c\| = \|\mathbf{K}_I\|$$

and the scalar product equality

$$\mathbf{K}\cdot\mathbf{U} = -k_{x_c}U_c + k_{z_{c0}}W_c = -k_{x_d}U_{xd} + \frac{m}{r}U_\theta$$

Then Eq. (11) can be expressed as

$$\acute{\Box}\,\Phi(x_c,y_c,z_c,t) = \left[-(\omega_{ex} + k_{x_c}U_c - k_{z_{c0}}W_c)^2/c_0^2 + k_{x_c}^2 + k_{y_c}^2 + k_{z_{c0}}^2 - i\frac{k_{z_{d0}}}{r}\right]\Phi(x_c,y_c,z_c,t), \tag{12}$$

whereas the expression directly obtained from Eq. (9) is

$$\acute{\Box}\,\Phi(x_c,y_c,z_c,t) = [-(\omega_{ex} + k_{x_c}U_c - k_{z_{c0}}W_c)^2/c_0^2 + k_{x_c}^2 + k_{y_c}^2 + k_{z_{c0}}^2]\Phi(x_c,y_c,z_c,t). \tag{13}$$

As a result, an additional term $-ik_{z_{d0}}/r$ arises in the Helmholtz operator when mapping the thin annular strip into a rectilinear planar strip. This term is basically ignored in the original rectilinear approximation. It is defined as a function of the wave number components in the reference frame of the rectilinear-cascade by the equation:

$$\frac{-ik_{z_{d0}}}{r} = \frac{i}{r}(Q_{i,31}k_{x_c} + Q_{i,32}k_{y_c} - Q_{i,33}k_{z_{c0}}) \tag{14}$$

Therefore introducing the following change of variables:

$$\begin{cases} k_{x_c} \to \tilde{k}_{x_c} = k_{x_c} + \dfrac{iQ_{i,31}}{2r} \\ k_{y_c} \to \tilde{k}_{y_c} = k_{y_c} + \dfrac{iQ_{i,32}}{2r} \\ k_{z_{c0}} \to \tilde{k}_{z_{c0}} = \left[k_{z_{c0}}^2 - \dfrac{iQ_{i,33}k_{z_{c0}}}{r} + \dfrac{1-Q_{i,33}^2}{(2r)^2}\right]^{1/2} \\ \omega \to \tilde{\omega}_g = \omega_g - \dfrac{iQ_{i,31}}{2r}U_c \end{cases} \tag{15}$$

leads to a classical Helmholtz operator with modified wavenumbers:

$$\acute{\Box}\,\Phi(x_c,y_c,z_c,t) = [\tilde{k}_{x_c}^2 + \tilde{k}_{y_c}^2 + \tilde{k}_{z_c}^2 - [\tilde{\omega}_g + \tilde{k}_{x_c}U_c]^2/c_0^2]\Phi(x_c,y_c,z_c,t)$$

which is better suited to include a "cylindrical" effect in a problem posed in the cascade Cartesian coordinates. Then the model is recast by using Eq. (12) instead of Eq. (13) in the analytical developments from Eq. (8). Let $\tilde{D}$ be the Fourier transform of the jump of velocity potential with respect to $\tilde{k}_{x_c}$. The velocity potential is expressed as

$$\phi(x_c,y_c) = \int_{-\infty}^{\infty}\int_{-\infty}^{\infty} \frac{i\left(\tilde{k}_{y_c} - \dfrac{iQ_{i,32}}{2r}\right)\tilde{D}(\tilde{k}_{x_c})e^{-ik_{x_c}x_c - i(\tilde{k}_{y_c} - iQ_{i,32}/2r)y_c}}{2\pi(\tilde{k}_{x_c}^2 + \tilde{k}_{y_c}^2 + \tilde{k}_{z_c}^2 - [\tilde{\omega}_g + \tilde{k}_{x_c}U_c]^2/c_0^2)} \sum_n e^{in(\sigma + k_{x_c}d + (\tilde{k}_{y_c} - iQ_{i,32}/2r)h)}\,d\tilde{k}_{x_c}\,d\tilde{k}_{y_c}. \tag{16}$$

The integral over k_{y_c} must be performed first. To simplify, the cascade is assumed with zero lean angle ψ, for which $Q_{i,32}=-\sin\psi=0$ and the parameters in original Glegg's problem are modified as

$$\tilde{\kappa}=\frac{\tilde{\omega}_g}{c_0\beta^2},\quad \tilde{\kappa}_e^2=\tilde{\kappa}^2-\left(\frac{\tilde{k}_{z_c}}{\beta}\right)^2,\quad \tilde{\rho}=\sigma+\tilde{\kappa}Md,$$

$$\tilde{\xi}=\tilde{k}_{x_c}-\tilde{\kappa}M=k_{x_c}+\frac{\mathrm{i}Q_{i,31}}{2r}-\tilde{\kappa}M,\quad \tilde{\zeta}=\pm\sqrt{[\tilde{\omega}_g+\tilde{k}_{x_c}U_c]^2/c_0^2-\tilde{k}_{x_c}^2-\tilde{k}_{z_c}^2}.$$

Note that $\tilde{\zeta}=\beta\sqrt{\tilde{\kappa}_e^2-\tilde{\xi}^2}$ but $\sigma+k_{x_c}d\neq\tilde{\zeta}+\tilde{\xi}d=\sigma+\tilde{k}_{x_c}d$. The following additional parameter is then defined as

$$\tilde{\tilde{\zeta}}=\tilde{\zeta}-\frac{\mathrm{i}Q_{i,31}d}{2r}.$$

It enables to write $\sigma+k_{x_c}d=\tilde{\tilde{\zeta}}+\tilde{\xi}d$ and then leads to a formalism very close to that proposed initially by Glegg [25] with

$$\tilde{\vartheta}_n=\sqrt{\tilde{\kappa}_e^2-\left(\frac{n\pi}{\beta h}\right)^2}\quad\text{and}\quad\tilde{\theta}_n=-\tilde{\vartheta}_n,\quad\forall n\geq 0$$

$$\tilde{\delta}_n=\tilde{\kappa}M+\tilde{\vartheta}_{n-1}\quad\text{and}\quad\delta_n=k_{x_c}(\tilde{k}_{x_c}=\tilde{\delta}_n)=\tilde{\kappa}M+\tilde{\theta}_{n-1}-\mathrm{i}\frac{Q_{i,31}}{2r},\quad\forall n\geq 1$$

$$\tilde{\varepsilon}_n=\tilde{\kappa}M+\tilde{\vartheta}_{n-1}\quad\text{and}\quad\varepsilon_n=k_{x_c}(\tilde{k}_{x_c}=\tilde{\varepsilon}_n)=\tilde{\kappa}M+\tilde{\vartheta}_{n-1}-\mathrm{i}\frac{Q_{i,31}}{2r},\quad\forall n\geq 1$$

$$\tilde{f}_q=\frac{\sigma+\tilde{\kappa}Md-2\pi q-\mathrm{i}Q_{i,31}\dfrac{d}{r}}{\sqrt{d^2+(h\beta)^2}}\quad\text{and}\quad\tilde{\eta}_q^{\pm}=-\tilde{f}_q\sin\chi_e\pm\cos\chi_e\sqrt{\tilde{\kappa}_e^2-\tilde{f}_q^2},\quad\forall q\in\mathbb{Z}$$

$$\lambda_q^{\pm}=k_{x_c}(\tilde{\xi}=\tilde{\eta}_q^{\pm})=\tilde{k}_{x_c}(\tilde{\xi}=\tilde{\eta}_q^{\pm})-\mathrm{i}\frac{Q_{i,31}}{2r}=\tilde{\kappa}M+\tilde{\eta}_q^{\pm}-\mathrm{i}\frac{Q_{i,31}}{2r},\quad\forall q\in\mathbb{Z}$$

$$\tilde{Z}=-\frac{\mathrm{i}\tilde{\xi}}{\pi}(\beta h\log(2\cos\chi_e)+\chi_e d).$$

In particular the Kernel function reads

$$j(k_{x_c})=\frac{\mathrm{i}\tilde{\zeta}}{4\pi}\sum_{n=-\infty}^{\infty}\mathrm{e}^{\mathrm{i}n(\sigma+k_{x_c}d)+\mathrm{i}\tilde{\zeta}|nh|}=\frac{\tilde{\zeta}\sin\tilde{\zeta}h}{4\pi[\cos(\tilde{\zeta}h)-\cos(\sigma+k_{x_c}d)]}.$$

Finally, the two splitting functions of the Kernel function J_+ and J_- are unchanged by substituting all the variables by the tilde variables:

$$J_+(k_{x_c})=\frac{\tilde{\kappa}_e\beta\sin\tilde{\kappa}_e h\beta}{4\pi(\cos\tilde{\kappa}_e h\beta-\cos\tilde{\tilde{\zeta}})}\frac{\prod_{l=0}^{\infty}(1-\tilde{\xi}/\tilde{\theta}_l)}{\prod_{q=-\infty}^{\infty}(1-\tilde{\xi}/\tilde{\eta}_q^-)}\mathrm{e}^{\tilde{Z}},$$

$$J_-(k_{x_c})=\frac{\prod_{l=0}^{\infty}(1-\tilde{\xi}/\tilde{\vartheta}_l)}{\prod_{q=-\infty}^{\infty}(1-\tilde{\xi}/\tilde{\eta}_q^+)}\mathrm{e}^{-\tilde{Z}}.$$

The zeros of J_+ are $(\delta_n)|_{n\geq 1}$, and those of J_- are $(\varepsilon_n)|_{n\geq 1}$. The poles of J_+ are in $\tilde{\xi}=\tilde{\eta}_q^-$, i.e. in $k_{x_c}=\lambda_q^-$, and those of J_- in $\tilde{\xi}=\tilde{\eta}_q^+$, i.e. in $k_{x_c}=\lambda_q^+$, for all $q\in\mathbb{Z}$.

To compute the scattered potential, the Fourier transform of the discontinuity of velocity potential $\tilde{D}$ must be determined. $\tilde{D}^{(1)}(\tilde{k}_{x_c})$ is unchanged with respect to $D^{(1)}(k_{x_c})$ in [25]. $J_-(-\omega_g/U)$ is computed by noting that $\tilde{\tilde{\xi}}_0=-\tilde{k}_{x_{c0}}-\tilde{\kappa}M=-k_{x_{c0}}-\mathrm{i}(Q_{i,31}/2r)-\tilde{\kappa}M$. The expressions of $D^{(2)}$, $D^{(3)}$, and $D^{(4)}$ are the same as in [25] with the tilde variables. The term A_c defined by Eq. (17) or (18) is then again introduced as was done in the original model [26] to derive the analytical formulation for the velocity potential or the pressure field inside the inter-blade channel and for the unsteady-blade loading:

$$A_c(k_{x_c})=+\frac{1}{2}\left\{\frac{\mathrm{e}^{\mathrm{i}\tilde{\zeta}y_c}}{1-\mathrm{e}^{\mathrm{i}\tilde{\zeta}h-\mathrm{i}k_{x_c}d-\mathrm{i}\sigma}}+\frac{\mathrm{e}^{-\mathrm{i}\tilde{\zeta}y_c}}{1-\mathrm{e}^{-\mathrm{i}\tilde{\zeta}h-\mathrm{i}k_{x_c}d-\mathrm{i}\sigma}}\right\}.\tag{17}$$

It can also be expressed as

$$A_c(k_{x_c})=-\frac{1}{2(\cos(\tilde{\zeta}h)-\cos(k_{x_c}d+\sigma))}[\underbrace{\mathrm{e}^{\mathrm{i}(k_{x_c}d+\sigma)}\cos(\tilde{\zeta}y_c)}_{(1)}\ \underbrace{-\cos(\tilde{\zeta}(y_c-h))}_{(2)}].\tag{18}$$

The model developments are then identical to those described initially by Glegg [25].

In the general case when $Q_{i,32}$ is non zero, the Kernel function j can no longer be obviously split into analytic functions in the upper and lower parts of the complex plane to yield a simple evaluation of Eq. (16).

The following Sections 3 and 4 are aimed at validating or pointing out the limits of the use of the modified rectilinear cascade model in a strip theory.

3. Strip-theory versus three-dimensional computations in benchmark configurations

In this section, the strip-theory model is compared to fully three-dimensional computations in the cases of high and low hub-to-tip ratio annuli with zero stagger angle and no-swirl mean flow as proposed by Hanson for the category 4 of the Third Computational Aeroacoustic benchmark [47]. The available three-dimensional results [54–58] were obtained with the lifting-surface models developed by Namba [27] and by Schulten [29,59] as well as with the three-dimensional-annular Linearized-Euler code of Atassi et al. [60] and the LINFLUX code (three-dimensional-annular Linearized-Euler code e.g. [61,62]). Some results are also compared with the two-dimensional and three-dimensional rectilinear cascade codes LINSUB and LINC, respectively. The former is based on Smith's model [17] and the latter on the developments by Goldstein [63] and Atassi and Hamad [64]. The investigated annular cascade is a stator with B_S=24 vanes, whose geometry is summarized in Table 1. The duct can be either a narrow annulus or a large annulus of hub-to-tip ratio H=0.98 or 0.5, respectively. The incident vortical gust is the harmonic of order p of the wakes of an upstream rotor of B_R blades with an angular rotation velocity Ω_R. The excitation is defined in the duct cylindrical coordinates (r,θ_d,x_d) as

$$v(r,\theta_d,x_d,t) = U_{xd} V_p \mathrm{e}^{\mathrm{i}[(pB_R\Omega_R x_d/U_d) + pB_R\theta_d + 2\pi q\tilde{r}] - \mathrm{i}pB_R\Omega_R t}, \tag{19}$$

where $\tilde{r} = (r-R_H)/(R_T-R_H)$ and the index q stands for the radial order of the excitation, with a radial variation of phase $2\pi q\tilde{r}$ and $\Omega_R = M_T c_0/R_T$, M_T being the tangential Mach number at the upstream rotor blade tip. All test cases correspond to the blade passage frequency fundamental p=1. The investigated radial orders q range from 0 to 3.

The pressure jump across a vane, the radiated pressure field and the modal coefficients are calculated with the present model and compared with the fully three-dimensional results and alternative rectilinear models available in the literature. The modal coefficients are defined at $x_d = -c$ and $2c$, and refer to the eigen functions in an annular duct with a uniform mean flow, normalized by their maximum amplitude. Since the leading edge of the stator vanes is at x_c=0, the two reference positions are located at one chord upstream and one chord downstream of the blade row, respectively. The corresponding modal amplitudes are defined by

$$C^{+}_{m,\mu}(\omega) = \frac{\gamma}{\rho_0 c_0^2} \max(E_{m,\mu}) \mathcal{P}^{+}_{m,\mu}(\omega) \mathrm{e}^{-\mathrm{i}k^{+}_{x,m\mu}c},$$

$$C^{-}_{m,\mu}(\omega) = \frac{\gamma}{\rho_0 c_0^2} \max(E_{m,\mu}) \mathcal{P}^{-}_{m,\mu}(\omega) \mathrm{e}^{+2\mathrm{i}k^{-}_{x,m\mu}c}. \tag{20}$$

3.1. Large hub-to-tip ratio H=0.98

The vane pressure jump, the pressure field and the modal coefficients are first calculated in a very narrow-annulus configuration with H=0.98 and q=0 for the four lowest tip Mach numbers in order to assess the strip-theory procedure in a case where three-dimensional effects are expected to be negligible. In such a case the rectilinear model is fully justified. In particular, the accuracy of the results is checked for cut-off, resonant and cut-on configurations. Indeed, as reported in the benchmark, the cascade is cut-off at the smallest tip Mach number M_T=0.3897. This means that no cascade mode is cut-on, and that the radiated acoustic field is exponentially decaying with axial distance away from the blade row. At M_T=0.4330 the annular cascade is excited exactly at its cut-on frequency, which means that it is at resonance. In this

Table 1
Definition of the stator geometry and parameters of the incident vortical gust.

B_R	B_S	H	χ (°)	φ (°)	ψ (°)	c	
16	24	0.98 or 0.5	0	0	0	$\frac{2\pi R_T}{B_S}$	
M_{xd}	M_T	$\overline{\omega}_{ex}$	p	$k_{z_{c0}}$	q	V_p	σ
0.5	0.3897 0.4330 0.4763 0.6485 0.7830	$\frac{pB_R M_T c}{R_T}$	1	$\frac{2\pi q}{(R_T-R_H)}$	0–3	0.1	$\frac{2\pi pB_R}{B_S}$

configuration, the pressure response can be very sensitive to the flow conditions. In the rectilinear model, in the particular case of zero sweep and stagger angles and zero spanwise wavenumber, the non-dimensional cut-on frequency of the cascade mode j is given by

$$\overline{\omega}_{\mathrm{ex},c,j} = \frac{\omega_{\mathrm{ex},c,j}c}{c_0} = \frac{\beta}{s}(\sigma - 2\pi j).$$

The value rigorously depends on the radial position since the distance between two adjacent leading-edges s varies linearly between $0.98c$ and c from hub to tip. As a result, the tip Mach number which corresponds to the cascade cut-on frequency varies between 0.4418 and 0.4330. The duct mode $(m,\mu)=(-8,0)$ is cut-on in the last two cases: M_T=0.4763 and 0.6495.

3.1.1. Unsteady vane loading

The unsteady vane-loading or pressure jump distribution along the vane chord as derived analytically [26] is compared in Fig. 3 with the three-dimensional linearized Euler code LINFLUX and the rectilinear semi-numerical code LINSUB for the tip Mach numbers M_T=0.3897 and 0.4330. The comparison for the tip Mach numbers M_T=0.4763 and M_T=0.6495 are performed with the three-dimensional linearized Euler code developed by Atassi et al. and the rectilinear semi-numerical code LINC.

The present model is in very close agreement with the two rectilinear models in all cases. It also agrees well with Atassi's three-dimensional-annular linearized Euler code, for the cut-on configurations of Figs. 3(c) and (d). The small remaining discrepancies close to the leading edge might be attributed to resolution issues in the Euler numerical method. They are small enough to have negligible effects on a broadband noise prediction. The agreement is also good with Prasad and Verdon results produced by the LINFLUX code, as shown in Fig. 3(a) in the cut-off case, which is a configuration a bit more difficult to model. Finally, a quite good agreement is found in the resonant case of Fig. 3(b). This is an important result since the prediction at this frequency is expected to be very sensitive with respect to small inaccuracies in the description of the geometry.

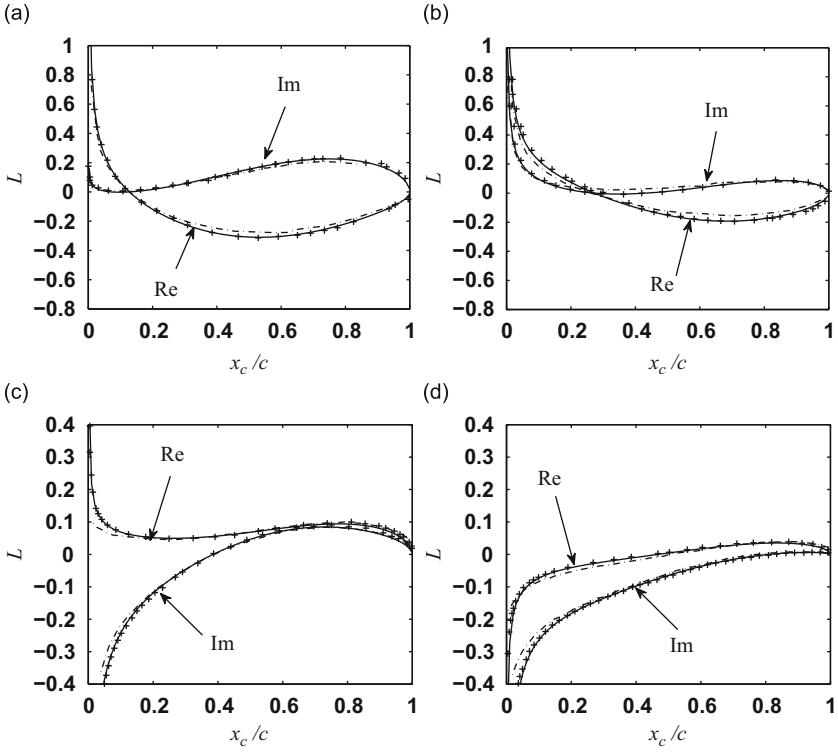

Fig. 3. Chordwise distributions of the real and imaginary parts of the unsteady vane loading made non-dimensional by $\rho_0 U_0^2/2$: $\mathcal{L}=\Delta\tilde{P}_{\mathrm{cd},0}(x_{\mathrm{cd}},R_m,\omega_{\mathrm{ex}})/(0.5\rho_0 U_0^2)$. (a, b) for an upwash $w_0=V_P U_{\mathrm{xd}}$ from the strip theory (——), Smith code (+) and the results of Prasad and Verdon with LINSUB code (—· —·) (e.g. [58]), for: (a) M_T=0.3897; (b) M_T=0.433. The results are obtained here for $\sigma=-2\pi B_R/B_S$ contrary to all other tested cases, in accordance with the definition in [58], and these results are the complex conjugate to those presented by [58] due to a different convention for the time Fourier transform. (c, d) for an upwash $w_0=V_P U_{xd}e^{-ik_{x_0}c/2}$ from the strip theory (——), Atassi's LINC model (+) and the three-dimensional Linearized-Euler Elhadidi and Atassi's code (—· —·) (e.g. [54]), for: (c) M_T=0.4763; (d) =0.6495.

3.1.2. Pressure field

The next step is to apply the acoustic analogy with the unsteady vane loading used as equivalent dipoles to predict the acoustic field radiated by an annular blade row; and to assess the accuracy of the predicted pressure field both inside and outside the annular blade row. This study is only performed in the cut-on configuration M_T=0.6495 where one mode is propagating upstream and downstream of the blade row.

The radiated field can be computed from the model in three different ways. The first two address the acoustic field produced by a rectilinear-cascade, in a two-dimensional geometry. Dealing with the most direct application, the model provides expressions for the velocity potential and then for the pressure field which are continuously valid outside and inside the inter-blade channel, without resorting to the equivalent sources of an acoustic analogy. Alternatively, according to the acoustic analogy, each vane acts as a chordwise distribution of dipoles, whose strength is defined by the pressure jump $\Delta\hat{P}_{\mathrm{cd},0}$. Calculating the radiated field in this way requires the two-dimensional Green's function for the convected Helmholtz equation with uniform flow. Green's function is written here as the complex conjugate of Lockard's expression [65] because a different convention for the time Fourier transform is chosen [26]. It is simply derived from the two-dimensional Green's function in a quiescent medium by applying the Prandtl–Glauert transformation:

$$G(x,y|\xi,\eta)=\frac{\mathrm{i}}{4\beta}\mathrm{e}^{-\mathrm{i}M_t k\check{x}/\beta^2}H_0^{(2)}\left(\frac{k}{\beta^2}\sqrt{\check{x}^2+\beta^2\check{y}}\right). \tag{21}$$

In the present case the mean-flow Mach number is M_t=M, the acoustic wave number $k=\omega_{\mathrm{ex}}/c_0$, $\check{x}=(x-\xi)$ and $\check{y}=(y-\eta)$ for a source point at (ξ,η) and an observer point at (x,y). The total field reconstructed by linear superposition of the contributions of all vanes assumed to radiate in free space must be identical to the direct prediction with the present uniformly valid extension of Glegg's solution. The periodicity of the cascade cannot be rigorously reproduced because the sum can only be made on a limited number of vanes B_S. Nevertheless the result in the vicinity of a reference channel $y_c\in[0,h[$ is reliable if B_S is large enough and if the vanes are distributed almost symmetrically on each side of this channel. These first two predictions must also compare favourably with those obtained from Smith's two-dimensional analysis [17], as suggested by Goldstein [18].

The third way of calculating the guided sound field deals with the actual annular-blade row configuration, using the strip theory approach. The principle is that the unsteady vane loading is computed on strips and the acoustic analogy is applied with Green's function tailored to the annular duct in uniform mean flow as stated in Section 2.1. In the narrow annulus configuration, this third formulation is not strictly speaking needed but it provides a good test case when comparing with both the two-dimensional rectilinear results and with the three-dimensional annular results obtained by Prasad and Verdon [58] with the LINFLUX code. Indeed, the results obtained in the case of a high hub-to-tip ratio annulus should be well reproduced by the solution of the rectilinear cascade having the local geometry of the annular cascade at mean radius R_m. Hence, the acoustic field predicted by the present strip theory will be compared with the rectilinear-cascade results of the code LINSUB.

The contours of the imaginary part of the pressure in the unwrapped cylindrical cut of the annulus are plotted in Fig. 4. The minus sign of the unsteady pressure field is plotted due to a convention for the time Fourier transform different from the one presented by [58], study from which the results with LINSUB and LINFLUX are extracted. The thick straight lines feature the stator vanes and the vertical dotted lines stand for the traces of the boundaries of the inter-vane channel. The fluid flows from left to right. The results for the propagating mode j=1 (i.e. $\sigma'=2\pi m/B_R=\sigma-2\pi j$, m=pB_R-jB_S=-8), previously obtained with the LINSUB and LINFLUX codes [58], are reported in Fig. 4(a). These reference calculations show a rather good overall agreement, even though the lines of constant values are slightly shifted from one computation to the other. The present rectilinear-cascade model matches Smith's results very well, as shown in Fig. 4(b). Next, Fig. 4(c) shows that the pressure field reconstructed from the two-dimensional acoustic analogy described above agrees quite well with the uniform analytical solution. Some discrepancies are seen upstream of the cascade presumably because of the truncation errors caused by the finite number of vanes. This confirms that in a two-dimensional context the acoustic pressure jump enables realistic sound predictions based on the acoustic analogy. Furthermore, this is also the case for the acoustic field predicted by the present strip theory in the actual high hub-to-tip ratio annulus, as shown by the pressure contours at the mean radius R_m in Figs. 4(d), (e) and (f). Indeed Fig. 4(d) reports the sole contribution of the cut-on duct modes, whereas Figs. 4(e) and (f) are obtained by adding the contributions of the first and the first five cut-off duct modes, respectively. The results stress the important role of the evanescent modes in local field close to the cascade. The field downstream of the blade row is almost governed by the cut-on mode (-8,0) only, as shown in Fig. 4(d) by the very good agreement with the LINSUB results. The agreement is also rather good upstream for $x_c/c<-0.5$. On the contrary, large discrepancies are found upstream, closer to the cascade ($x_c/c\in[-0.5,0]$) and inside the channel. Including the first cut-off mode in Fig. 4(e) enables to capture the correct behaviour in the region closely upstream of the cascade, and in the inter-blade channel, except near the leading-edge of the upper vane where discrepancies are notably reduced but remain noticeable. Finally, adding four cut-off modes more further improves the results, as shown in Fig. 4(f). The strip-theory is now in good agreement with rectilinear-cascade models, the small remaining discrepancies in the very vicinity of the vanes stressing the high sensitivity of the response to the first cut-off modes.

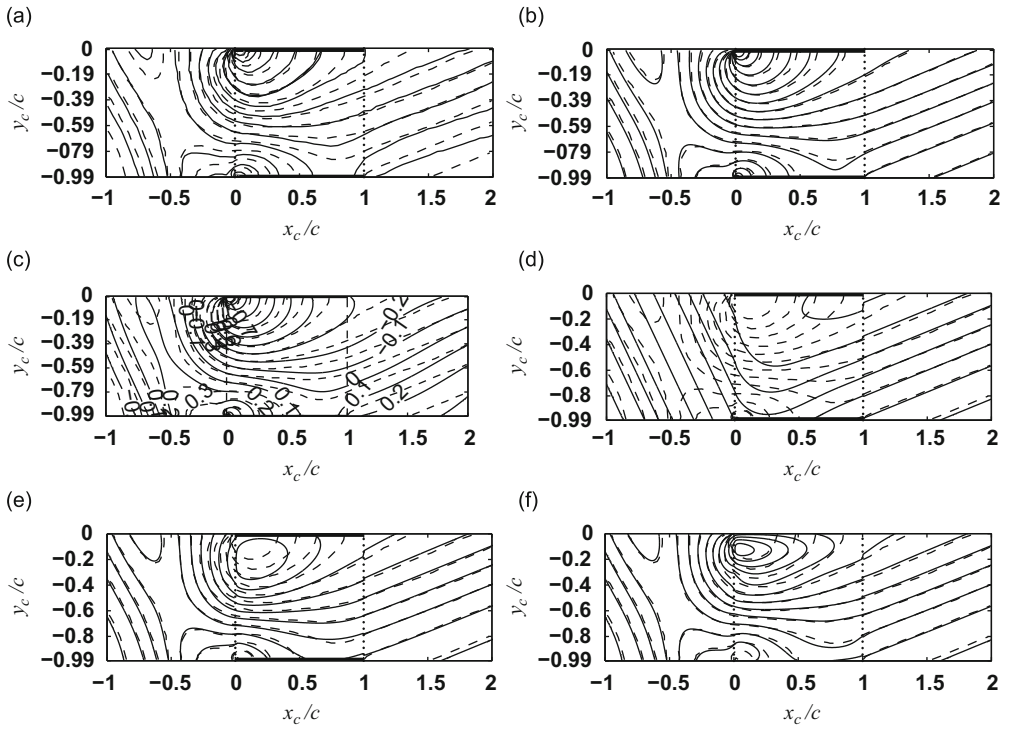

Fig. 4. Opposite of the imaginary part of the unsteady pressure field at midspan R_m made non-dimensional by $\rho_0 V_p U_{xd}^2$ for the test case defined in Table 1 with H=0.98, and a two-dimensional gust (i.e. q=0) at M_T=0.6495 obtained with: (a) Smith's linear two-dimensional model (black dashed lines) and the three-dimensional Euler linearized LINFLUX code (black solid lines) from [58]; (b) the present model computed directly without the unsteady vane loading [26] (black lines) and Smith's linear two-dimensional model (black dashed lines); (c) a two-dimensional acoustic analogy for a rectilinear cascade using the unsteady vane loading produced by the present model as equivalent dipole sources (black lines); (d–f) an analogy acoustic for an annular cascade using the unsteady vane loading produced by the present model as equivalent dipole sources (black lines) and Smith's model (dashed lines) with the computation of the contribution in the strip theory of: (d) solely the cut-on mode (-8,0), (e) the cut-on mode (-8,0) and the first cut-off mode ((16,0)), (f) the cut-on mode (-8,0) and the first 5 cut-off modes ((16,0), (-32,0) (40,0), (-56,0), (64,0)).

Table 2
Real and imaginary parts of the acoustic pressure mode $(m,\mu)=(-8,0)$ in the plane $x_d=-c$ upstream of the stator from Namba's method, Schulten's, Elhadidi and Atassi's models, the strip theory and the rectilinear cascade model, for M_T=0.3897, 0.433, 0.4763 and 0.6495.

M_T	0.3897	0.4330	0.4763	0.6495
Namba	$-5.067e^{-3}$ + $1.924e^{-3}$ i	$-1.142e^{-3}-2.170e^{-4}$ i	$-7.603e^{-3}+1.837e^{-3}$ i	$7.577e^{-3}-1.814e^{-3}$ i
Schulten	$-5.407e^{-3}+2.231e^{-3}$ i	$2.083e^{-3}+3.459e^{-4}$ i	$-7.538e^{-3}+2.055e^{-3}$ i	$7.364e^{-3}-2.453e^{-3}$ i
Elhadidi and Atassi	NC	NC	$-7.768e^{-3}+3.439e^{-3}$ i	$7.027e^{-3}-3.863e^{-3}$ i
Strip-theory	$-5.751e^{-3}+2.476e^{-3}$ i	$-4.023e^{-3}-5.897e^{-4}$ i	$-7.060e^{-3}+1.605e^{-3}$ i	$7.106e^{-3}-2.089e^{-3}$ i
Rectilinear model	$-5.773e^{-3}+1.348e^{-3}$ i	$-1.575e^{-3}-4.342e^{-4}$ i	$-7.481e^{-3}+1.643e^{-3}$ i	$7.319e^{-3}-2.390e^{-3}$ i

Table 3
Real and imaginary parts of the acoustic pressure mode $(m,\mu)=(-8,0)$ in the plane $x_d=2c$ downstream of the stator from Namba's method, Schulten's, Elhadidi and Atassi's models, the strip theory and the rectilinear cascade model, for M_T=0.3897, 0.433, 0.4763 and 0.6495.

M_T	0.3897	0.4330	0.4763	0.6495
Namba	$8.584e^{-3}-4.532e^{-3}$ i	$1.175e^{-2}-5.298e^{-3}$ i	$1.050e^{-2}+1.604e^{-2}$ i	$-1.120e^{-2}+5.684e^{-3}$ i
Schulten	$8.734e^{-3}-4.943e^{-3}$ i	$3.410e^{-3}-6.891e^{-4}$ i	$1.061e^{-2}+1.556e^{-2}$ i	$-9.946e^{-3}+5.870e^{-3}$ i
Elhadidi and Atassi	NC	NC	$1.217e^{-2}+1.497e^{-2}$ i	$-9.665e^{-3}+6.577e^{-3}$ i
Strip-theory	$8.728e^{-3}-5.095e^{-3}$ i	$1.849e^{-2}-6.206e^{-3}$ i	$1.042e^{-2}+1.521e^{-2}$ i	$-9.570e^{-3}+5.713e^{-3}$ i
Rectilinear model	$9.500e^{-3}-3.116e^{-3}$ i	$1.881e^{-4}-1.786e^{-2}$ i	$1.084e^{-2}+1.526e^{-2}$ i	$-9.870e^{-3}+5.920e^{-3}$ i

3.1.3. Duct mode amplitude

Finally, the complex amplitude of the duct mode $(m,\mu)=(-8,0)$, defined in Eq. (20), is computed with the present model both from Glegg's original formulation and from the strip theory and compared with the prediction obtained by the

three-dimensional lifting-surface predictions of Namba [27] and Schulten [29,59], as well as with the three-dimensional-annular Linearized-Euler code of Atassi et al. [60]. All results are reported in Tables 2 and 3, giving the upstream and downstream radiations, respectively, for the four values of the tip Mach numbers M_T.

The results obtained in the two cut-on configurations with the present model are within the dispersion range of the three-dimensional predictions, a slight under-prediction remaining with the strip theory. Indeed, small variations are observed in all the results, especially for the downstream coefficients in Table 3, mostly caused by the difficulty to apply proper outflow conditions in the numerical simulations [54]. Besides, the present rectilinear-cascade model and its strip-theory application provide very similar self-consistent results.

In the cut-off case, M_T=0.3897, the strip theory remains in good agreement with the three-dimensional lifting-surface models of Namba and Schulten. Thus it applies at low frequencies as well. The rectilinear-cascade model provides the correct result upstream and consistent absolute values downstream despite a small discrepancy in phase. In the resonant case, M_T=0.4330, the results obtained from the two three-dimensional lifting-surface models are very different, in particular downstream where Schulten's results are smaller than those obtained by Namba. This difference emphasizes the difficulty to accurately predict the behaviour at resonance. The strip theory provides results closer to those of Namba downstream, though significantly different, and values 2–3 times larger upstream. Globally, the results obtained with the rectilinear-cascade model are consistent with the lifting-surface models with respect to upstream propagation, whereas downstream, it is almost out-of-phase when comparing with Namba's model and the strip theory. Finally, the prediction at resonance remains a tricky issue which should be born in mind in the future.

3.2. Small to moderate hub-to-tip ratio H=0.5

The exhausts of real fan engines typically involve much smaller hub-to-tip ratios H of about 0.3–0.6. For further assessment of the model, the comparisons are now discussed for the value H=0.5 and a three-dimensional incident gust with $q \in [0,3]$ at a tip Mach number of M_T=0.783. At the corresponding angular frequency ($\overline{\omega}_{\mathrm{ex}} = 3.28$, i.e. $\tilde{\omega}_{\mathrm{ex}} = \omega_{\mathrm{ex}} R_T/c_0 = 12.53$) two duct-modes are cut-on and excited by the rotor-stator according to Tyler and Sofrin's criterion [66]: $(m,\mu) = (-8,0)$ and $(m,\mu) = (-8,1)$.

The incident gust defined by Eq. (19) for an annular blade row must be converted at each strip of mean radius r to an equivalent harmonic gust in the local rectilinear cascade reference frame having the local geometry of the annular blade row, bearing in mind that the span is assumed infinite in the strip-theory model for the sake of calculating the induced lift. The calculation is performed at radius r (i.e. in $\mathbf{x}_{d\,0}$ at time t_0). Let us define the local cascade reference frame $\mathcal{R}_{\mathrm{cd}}$ with its origin O_{cd} at radius r. In this reference frame z_{cd} is the local radial coordinate extending below and above r and exactly zero at r. Introducing

$$v(r,\theta_d,x_d,t) = V_p \mathrm{e}^{\mathrm{i}[(pB_R\Omega_R x_d/U_{xd}) + pB_R\theta_d + 2\pi q\tilde{r}] - \mathrm{i}pB_R\Omega_R t} = V_p \mathrm{e}^{\mathrm{i}2\pi q\tilde{r}}\, \mathrm{e}^{\mathrm{i}[(pB_R\Omega_R x_d/U_{xd}) + pB_R\theta_d + 2\pi q z_{\mathrm{cd}}/(R_T - R_H)] - \mathrm{i}pB_R\Omega_R t},$$

with z_{cd}=0, the unsteady response on vane of indices 0, $\Delta P_0(\mathbf{x}_{d0},t_0)$, is the rectilinear-cascade response to an incident gust of spanwise wavenumber:

$$k_{z_{c0}} = \frac{2\pi q}{(R_T - R_H)},$$

of incident complex velocity amplitude: $w_0 = V_p \mathrm{e}^{\mathrm{i}2\pi q\tilde{r}}$ and with $(\omega, k_{x_{c0}}, \sigma) = (pB_R\Omega_R, \omega/U_d, 2\pi pB_R/B_S)$. Its temporal Fourier transform written in the cascade reference frame $\mathcal{R}_{\mathrm{cd}}$ is $\Delta\hat{P}_{\mathrm{cd},0}(x_{\mathrm{cd}}, r_0, \omega_{\mathrm{ex}})$.

3.2.1. Unsteady vane loading

First a two-dimensional gust (q=0) is considered. The chordwise variation of the unsteady vane loading produced at duct mid-height R_m is plotted in Fig. 5. Unlike with a narrow-annulus configuration, the difference with three-dimensional annular models is no longer negligible and locally reaches up to 34 percent for the imaginary part at x_c=0.27c. Yet the agreement remains acceptable in terms of overall shape and levels for both real and imaginary parts of the unsteady vane loading, especially for the sake of fan broadband noise prediction. Therefore the investigation is extended to the three-dimensional incident gusts of indices q=1 and 3, respectively. The radial variation of the unsteady vane loading produced by the rectilinear-cascade formulation without correction is obviously unrealistic. Indeed large discrepancies with alternative prediction are shown in Fig. 6. Similar results are found at different chordwise locations. The radial amplitude variations of the unsteady vane loading are over-estimated and the rectilinear-cascade model exhibits too many radial nodes. These discrepancies are attributed to three-dimensional effects not-accounted for in the strip theory: the modal scattering on radial orders, the effect of rigid wall boundaries, the non-coincidence of the cut-on frequencies of the annular duct modes and the rectilinear-cascade modes, or the non-parallelism of the vanes. For instance, contrarily to the present strip theory, Schulten's model ensures zero radial derivatives at the walls by using cosine functions and Namba's model involves functions which satisfy the same condition.

Similar problems are observed for an incident gust with a higher radial wavenumber (q=2 or even q=3, i.e. $k_{z_{c0}} c = 9.87$) in Fig. 8. Moreover the unsteady vane loading drops off too rapidly for $x_c \geq 0.5c$ when compared with the three-dimensional computations in Figs. 7 and 8 for q=2 and 3, respectively. Introducing a non-zero radial wavenumber of the incident gust lowers the cut-on frequencies of the cascade modes. In particular, for the present case, $k_{zc\ 0}c$ is large and the

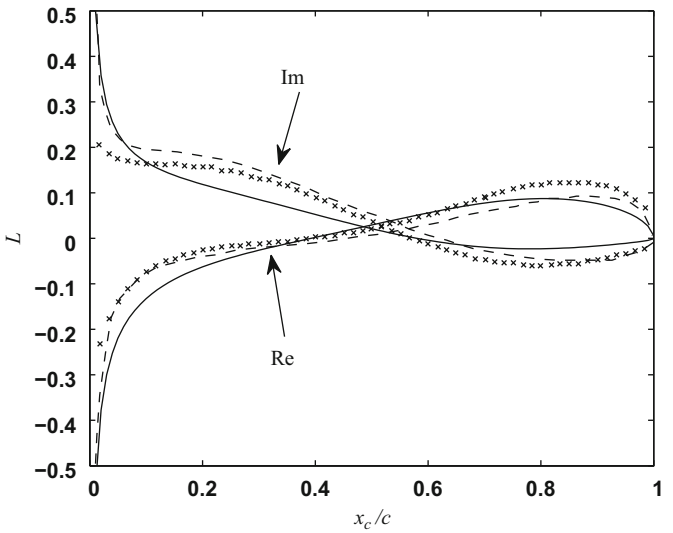

Fig. 5. Chordwise distributions of the real and imaginary parts of the unsteady vane loading at duct mid-span R_m made non-dimensional by $\rho_0 U_0^2/2$: $\mathcal{L}=\Delta\hat{P}_{cd,0}(x_{cd},R_m,\omega_{ex})/(0.5\rho_0 U_0^2)$, from the strip theory (——), from Schulten's model (— — —) and from Atassi et al.'s three-dimensional Linearized-Euler code (·) (results of three-dimensional models from [54]), for $q=0$.

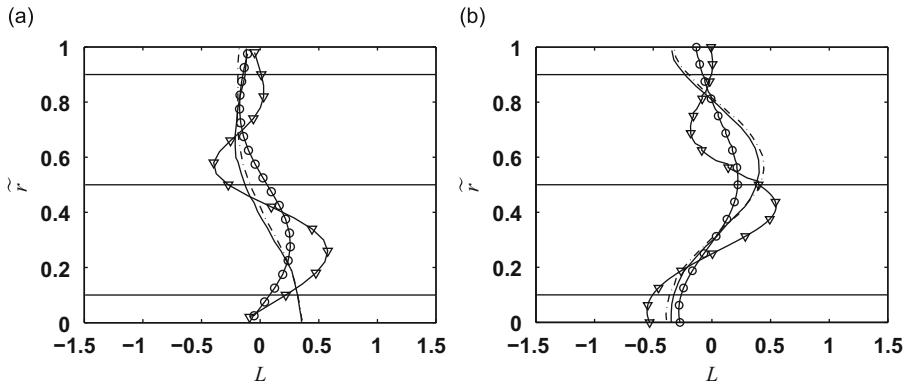

Fig. 6. Radial distribution of the real (a) and imaginary parts (b) of the unsteady vane loading at $x_c=0.1c$ made non-dimensional by $\rho_0 U_0^2/2$: $\mathcal{L}=\Delta\hat{P}_{cd,0}(x_{cd},R_m,\omega_{ex})/(0.5\rho_0 U_0^2)$, from the strip theory with the original unsteady vane loading (—▽—) and with the corrected unsteady vane loading presented in 2.3 (—○—), from Schulten's model (——) and from Atassi et al.'s three-dimensional Linearized-Euler code (— — —) (results of three-dimensional models from [57]).

cut-on frequencies of the rectilinear are drastically increased. For $q=0$ a cascade-mode is cut-on whereas for $q=1$ all modes are cut-off and for $q=3$ the modes are cut-off and the studied frequency is even farther from the cut-on frequencies. As a result, the rectilinear-cascade model concentrates the unsteady loading near the leading-edge, which is much less pronounced in three-dimensional annular models as shown in Fig. 8.

Taking the correction of Section 2.3 into account is now investigated for $q=1$ and 3 and the calculations are pointed with circle markers in Fig. 6. The results for two-dimensional gusts are unchanged for unswept cascades from Eq. (15). The correction significantly improves the prediction of the radial distribution of the unsteady vane loading for $q=1$, both in shape and level: the number of radial nodes is reduced, and the overall unsteady loading amplitude decreases. As for $q=1$ differences still remain, mainly near the walls, as the radial derivative of the pressure jump is not set to zero in the present model. The corrected results for higher radial wavenumbers ($q=3$) are found to make no significant difference with the original ones. In this case the real part of the corrected spanwise wavenumber $\tilde{k}_{z_{c0}}$ is slightly larger than $k_{z_{c0}}$, and the small variation in radial wavenumber has very little effect.

3.2.2. Pressure field

The pressure field radiated both inside and outside the annular blade row is plotted as in Section 3.1.2 now for $M_T=0.783$, $H=0.5$, and $q=0$ or 1 in Figs. 9 and 10. The minus sign of the unsteady pressure field is plotted due to a convention for the time Fourier transform different from the one presented by [58], study from which the results with LINSUB and LINFLUX are extracted. Again, the rectilinear-cascade model prediction matches Smith's results very well, as

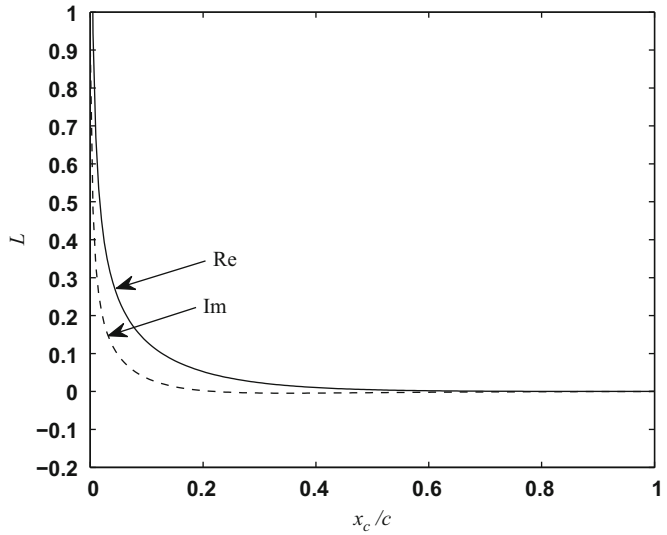

Fig. 7. Chordwise distributions of the real (——) and imaginary (— — —) parts of the unsteady vane loading at duct mid-span R_m made non-dimensional by $\rho_0 U_0^2/2$: $\mathcal{L}=\Delta\hat{P}_{cd,0}(x_{cd},R_m,\omega_{ex})/(0.5\rho_0 U_0^2)$, from the strip theory, for q=2.

shown in Fig. 9(a) for q=0. But it strongly differs from the one obtained with the three-dimensional Euler linearized code LINFLUX, plotted in Fig. 9(b). Even if the excitation is in phase from hub to tip, the low hub-to-tip ratio induces significant differences with the two-dimensional response. Fig. 9(d) shows that the strip-theory approach is in better agreement with the three-dimensional linearized Euler results upstream and downstream of the blade row, because it allows synthesising the correct annular-duct modes. Again, the cut-on modes provide the correct behavior away from the cascade as seen in Fig. 9(c), but the first cut-off modes contributions must be included to be closer to the behaviour near and inside the blade row as shown in Fig. 9(d). The largest discrepancies again occur in the vane passage. They are mostly attributed to numerical errors and to the difficulty of applying the acoustic analogy inside the inter-blade channel in the close vicinity of the sources. Larger discrepancies are also expected at the tip radius caused by the end-wall effects.

The response to a three-dimensional excitation is then investigated for q=1 in Fig. 10. Applying the correction (Fig. 10(b)) produces a phase shift of one inter-blades channel compared to the uncorrected results in Fig. 10(a). The patterns of the pressure field are a bit modified, in particular upstream, due to a new distribution of the radiated energy on the propagating duct modes. Essentially the overall amplitudes are decreased and the iso-value contours are more spaced out.

When these results are compared with the ones for a two-dimensional excitation (q=0) in Fig. 9(d), the amplitudes predicted by the strip-theory are higher in the three-dimensional case (q=1) than in the two-dimensional case (q=0), with an increase by about a factor two for the uncorrected unsteady vane loading. The accuracy of this behaviour and the actual effect of the correction will be discussed in the next section by comparison with three-dimensional models. In addition, the pressure patterns are notably different in Figs. 9(d) and 10(b), particularly in the inter-blade regions and farther downstream. The cut-on and cut-off duct modes are unchanged since the same incident frequency is assumed. But the incident radial wavenumber modifies the unsteady vane loading distribution, both along the chord and the span. Consequently the coupling between the source field in the blade row and the radiation term is modified. Indeed here, the mode $(m,\mu)=(-8,1)$ dominates upstream for both gusts (q=0 and 1), whereas downstream the dominating mode is $(m,\mu)=(-8,0)$ for q=0 and $(m,\mu)=(-8,1)$ for q=1 as will be observed in Figs. 11 and 12 of Section 3.2.3.

3.2.3. Duct mode amplitude

This section is aimed at assessing whether the differences pointed out in Section 3.2.1 lead to errors in predicting the coefficients of the cut-on duct modes when resorting to the strip theory on the one hand, and the effectiveness of the correction on the other hand. The modal coefficients defined in Eq. (20) obtained with the present model are plotted in Figs. 11, 12, 13 and 14 for q=0–3, respectively, and compared with the coefficients obtained with Namba's and Schulten's lifting surface models. The original model is shown in black-striped bars and the corrected one in black bars. As seen in Fig. 11, for a two-dimensional gust (q=0), the energy distribution between upstream and downstream is erroneous: indeed the duct mode $(-8,0)$ is under-estimated and the mode $(-8,1)$ over-estimated upstream, and vice versa downstream. The correction does not modify this case as expected.

In Fig. 12, the main concern is the over-estimated response of the mode $(m,\mu)=(-8,1)$ when the radial mode order of the excitation is $q=\mu=1$. The correction reduces the amplitude of the duct mode $(m,\mu)=(-8,1)$ by about 20 percent

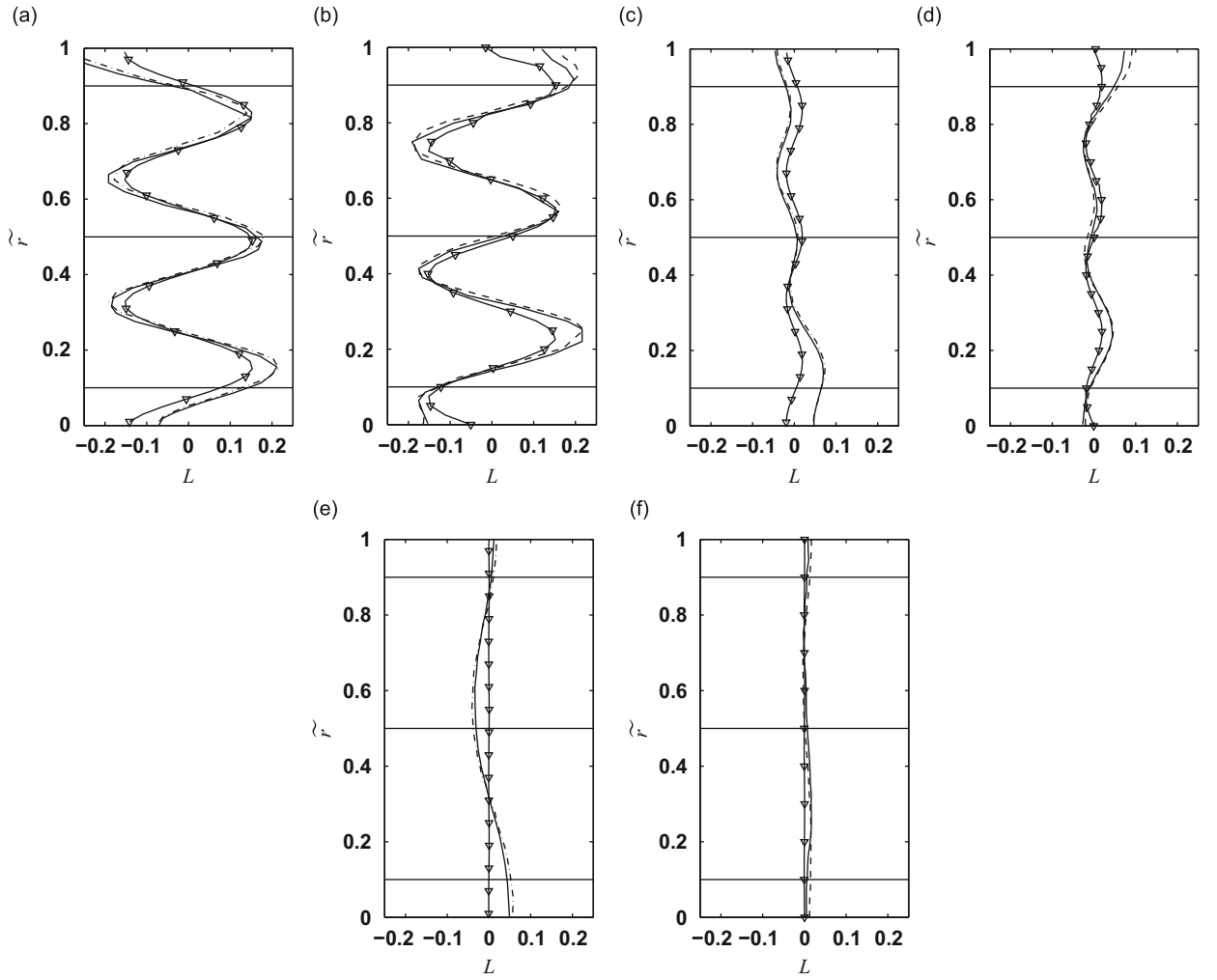

Fig. 8. Radial distribution of the real (a–c–e) and imaginary (b–d–f) part of the unsteady vane loading made non-dimensional by $\rho_0 U_0^2/2$: $\mathcal{L} = \Delta\hat{P}_{cd,0}(x_{cd},R_m,\omega_{ex})/(0.5\rho_0 U_0^2)$, from the strip theory with the original unsteady vane loading (—▽—), from Schulten's model (——) and from Atassi et al.'s three-dimensional Linearized-Euler code (— — —), for q=3 at: (a, b) x_c=0.06c; (c, d) x_c=0.2c; (e, f) x_c=0.5c (results of three-dimensional models from [57]).

downstream and 35 percent upstream. Yet, the amplitudes remain 3–4 times too high. These issues are mainly due to the fact that the rectilinear model does not predict scattering in radial mode orders. If the radiated field is computed directly without resorting to the unsteady vane loading at each radius, the radiated modes all have the radial order of the incident mode. If the strip theory is considered, the acoustic analogy applied with Green's function tailored to the rigid annular duct distributes energy on all cut-on excited modes, according to Tyler and Sofrin's criterion. But, since the dipole sources are predicted by the rectilinear-cascade model, they are only approximate. In particular, ignoring the scattering in radial wavenumber in rectilinear cascade also induces errors in the unsteady vane loading prediction. As a result, the strip theory can still yield a wrong modal distribution. Additional errors can be observed in particular cases in which the number of cut-on duct modes and cut-on cascade modes is not the same everywhere or locally along the span, due to the non-coincidence of the cut-on frequencies. A correction of this issue has been proposed in a broadband noise context [67].

In Fig. 13, for the excitation with the higher radial order q=2, the strip-theory model is in better agreement with three-dimensional annular ones. In Fig. 14, the strip theory under-estimates the acoustic field for the highest radial wavenumber (q=3) and the correction brings no significant improvement. This is consistent with the prediction of the pressure-jump drop for $x/c \geq 0.5$, previously mentioned in Fig. 8.

Therefore, the inaccuracy of the unsteady vane loading as obtained from the original model (black stripes), leads to large errors in the coefficients of the two propagating duct modes and the correction only brings significant improvements for the case q=1. The correction proposed in Section 2.3 is mostly driven by the corrected expression of the spanwise wavenumber $\tilde{k}_{z_{c0}}$. It is defined by the square root of a complex term, the imaginary part of which is crucial since it is the corrected factor for an unswept cascade ($Q_{i,33}$=1). On the contrary, the imaginary part of the resulting wavenumber $\tilde{k}_{z_{c0}}$ has little effect in the tested configurations.

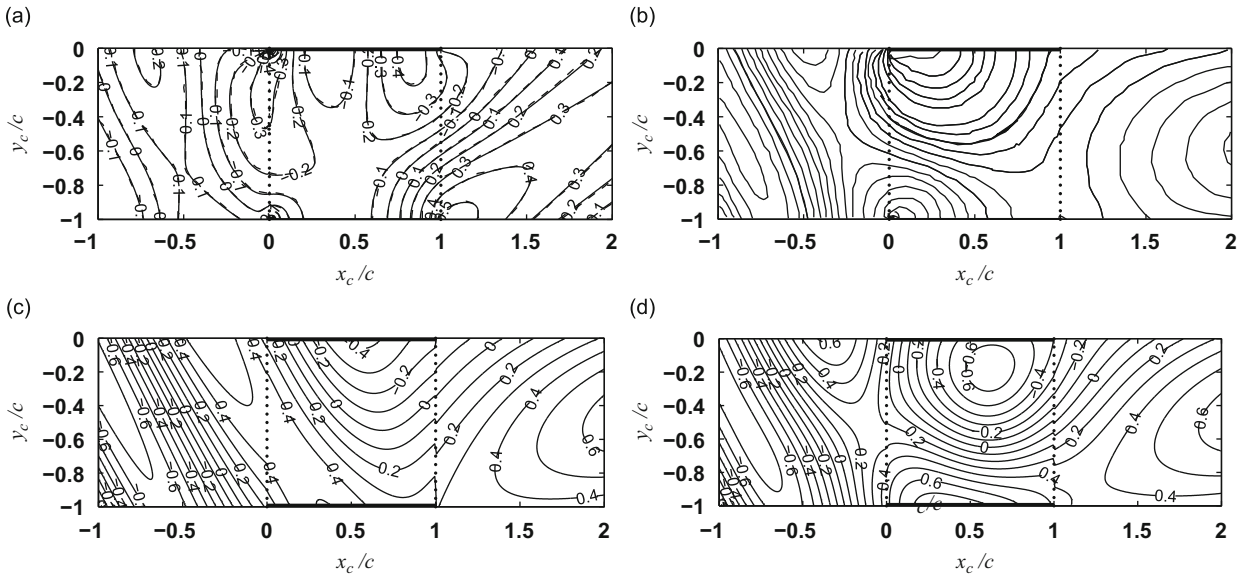

Fig. 9. Opposite of the imaginary part of the unsteady pressure field made non-dimensional by $\rho_0 V_p U_{xd}^2$ at tip radius R_T for the test case defined in Table 1 with H=0.5, and a two-dimensional gust (i.e. q=0) at M_T=0.873 obtained with: (a) the present model computed directly with no need for computation of the unsteady vane loading [26] (lines) and Smith's linear two-dimensional model (dashed lines); (b) the three-dimensional Euler linearized LINFLUX code; (c,d) an analogy acoustic for an annular cascade using the unsteady vane loading produced by the present model as equivalent dipole sources, with the computation of the contribution of: (c) solely the cut-on modes ((−8,0) and (−8,1)) and (d) the cut-on modes ((−8,0) and (−8,1)) and of the first four cut-off modes ((16,0), (−8,2) (16,1), (−8,3)).

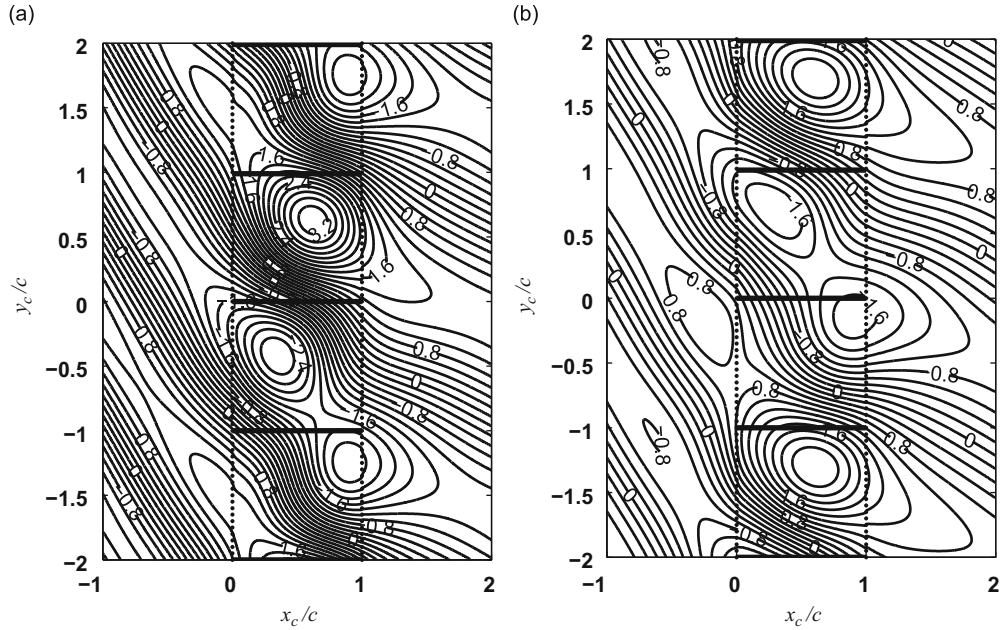

Fig. 10. Opposite of the imaginary part of the unsteady pressure field at tip radius R_T made non-dimensional by $\rho_0 V_p U_{xd}^2$ for the test case defined in Table 1 with H=0.5, and a three-dimensional gust (q=1) at M_T=0.873 obtained with the strip theory with the computation of the contribution of the cut-on modes ((−8,0) and (−8,1)) and of the first four cut-off modes ((16,0), (−8,2) (16,1), (−8,3)), resorting to: (a) the original rectilinear cascade response; (b) the corrected rectilinear cascade response of Section 2.3. The contours are plotted with a step of 0.2.

4. Application to a broadband fan noise problem

The extended formulation is dedicated to future implementation in a fan broadband noise prediction tool in an industrial context. Analytical models then remain a reasonable alternative to numerical simulations to determine the whole power spectral density of the acoustic radiated field. Nevertheless, more accurate prediction schemes are now

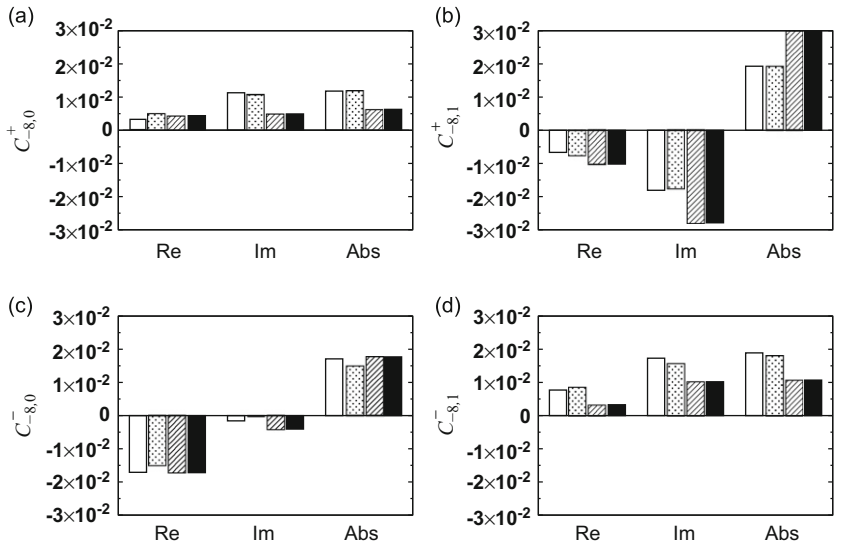

Fig. 11. Real and imaginary parts, and amplitude of the acoustic coefficients of the propagating modes $(m,\mu)=(-8,0)$ ((a) and (c)), and $(m,\mu)=(-8,1)$ ((b) and (d)) upstream (a, b) and downstream (c, d), for the incident radial mode orders $q=0$ from Namba's model (white), Schulten's (grey), initial (black stripes) and modified strip theory (black).

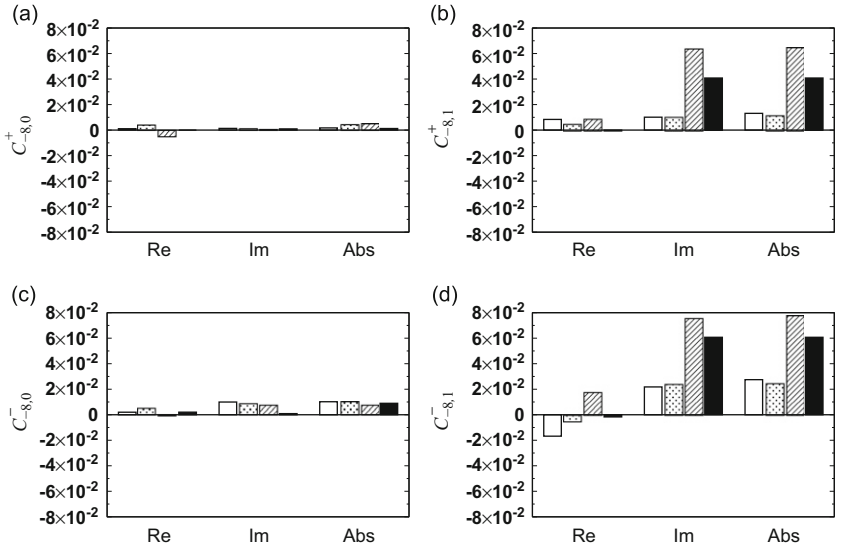

Fig. 12. Real and imaginary parts, and amplitude of the acoustic coefficients of the propagating modes $(m,\mu)=(-8,0)$ ((a) and (c)), and $(m,\mu)=(-8,1)$ ((b) and (d)) upstream (a, b) and downstream (c, d), for the incident radial mode orders $q=1$ from Namba's model (white), Schulten's (grey), initial (black stripes) and modified strip theory (black).

needed to reproduce the relative and absolute effects of the geometrical parameters of a fan, such as blade twist, sweep and lean in three-dimensional configurations, and the three-dimensional effects of the incident turbulence and the swirling mean flow effect [60]. The present strip theory approach is then developed to introduce main three-dimensional effects while resorting to semi-analytical model. It is then expected to be a good trade-off between analytical rectilinear cascade models dealing with three-dimensional incident gusts, semi-analytical strip-theory models resorting to two-dimensional unsteady blade-loading response and fully three-dimensional numerical simulations. The present strip theory approach is then used, resorting to the original or the corrected expression of the unsteady blade loading to predict the wake-interaction broadband noise of the 22-in source diagnostic test (SDT) fan rig of the NASA Glenn Research Center [49,48,50,51] with the baseline outlet guide vanes of 54 radial vanes in approach condition and is compared with the experimental results [51,41,68] in Fig. 15. The turbulence is assumed to be locally homogeneous, i.e. homogeneous on each strip and an isotropic Liepmann turbulence model is used. As proposed by Nallasamy and Envia [41] the turbulence is split

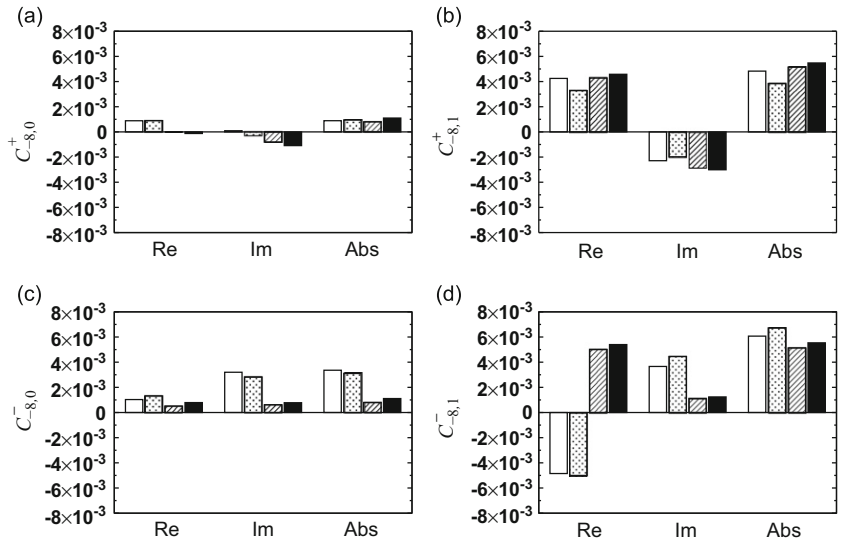

Fig. 13. Real and imaginary parts, and amplitude of the acoustic coefficients of the propagating modes $(m,\mu)=(-8,0)$ ((a) and (c)), and $(m,\mu)=(-8,1)$ ((b) and (d)) upstream (a, b) and downstream (c, d), for the incident radial mode orders q=2 from Namba's model (white), Schulten's (grey), initial (black stripes) and modified strip theory (black).

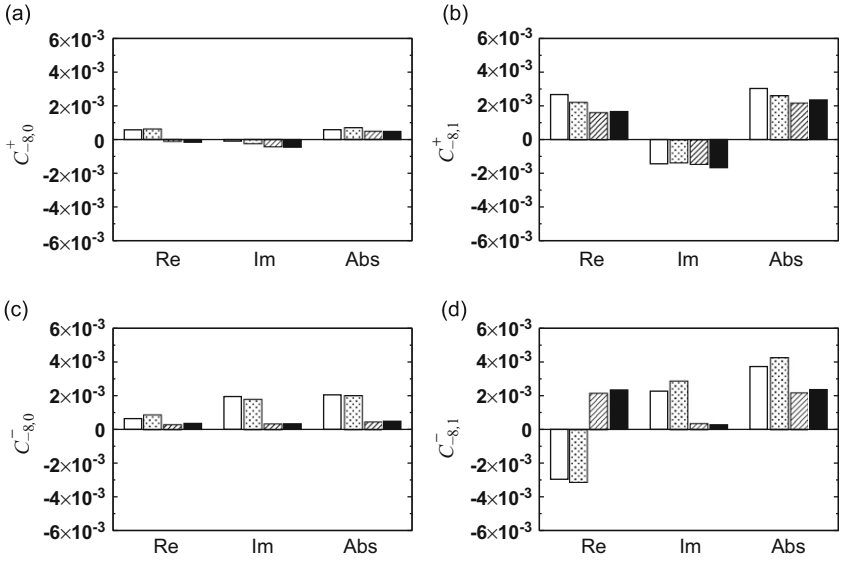

Fig. 14. Real and imaginary parts, and amplitude of the acoustic coefficients of the propagating modes $(m,\mu)=(-8,0)$ ((a) and (c)), and $(m,\mu)=(-8,1)$ ((b) and (d)) upstream (a, b) and downstream (c, d), for the incident radial mode orders q=3 from Namba's model (white), Schulten's (grey), initial (black stripes) and modified strip theory (black).

into the sum of a background component and a component from the turbulent rotor wakes which is assimilated to a random term multiplied by a gaussian distribution function to define the pitchwise variation of the turbulent wakes. The input data are provided by Envia et al. [41,48–51], and the broadband noise model is detailed in [69].

The results of the present model are plotted in Fig. 15 and compared with the experimental results from NASA (thick line), and the results from the code of Nallasamy and Envia [41] (symbols). The strip-theory model correctly predicts the shape of the spectrum and the central frequency of the broadband hump. Yet upstream, the levels are overpredicted by 1–3 dB, in the frequency range $f \in [2300,6500]$ Hz when the initial formulation with the original unsteady blade loading is used. The correction presented in Section 2.3 improves the results by reducing the overprediction of the hump, and by slightly decreasing the other parts of the spectrum. Therefore, the present model provides consistent predictions in this realistic turbomachinery configuration involving the rotor–stator interaction-noise mechanism as it captures the overall

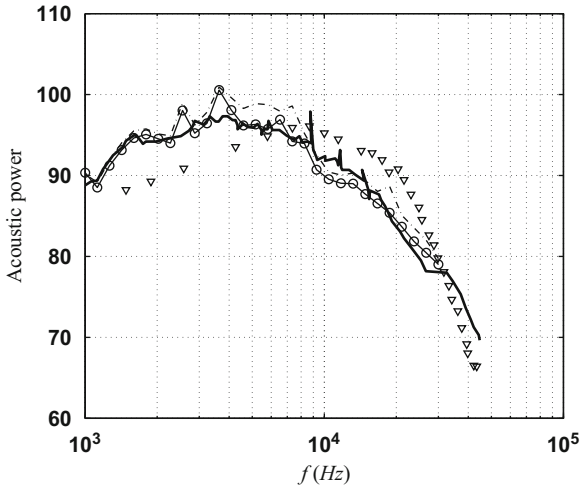

Fig. 15. Comparison of the spectra of narrow band acoustic power radiated upstream obtained experimentally by NASA [41] (▬▬), from the model developed by Nallasamy and Envia [41] (▽), from the present model with the original unsteady blade loading (▬·▬·), and with the modified unsteady blade loading (▬θ▬).

level and the shape of the measured spectrum well. In addition, the correction of the unsteady blade loading response of the rectilinear cascade introduces the main effect of the actual wave equation and then improves the prediction of the level.

5. Concluding remarks

A strip theory approach based on a previously published formulation for the unsteady blade loading produced by a rectilinear cascade has been derived. The unsteady blade loading evaluated, for each cylindrical strip, by the rectilinear cascade model for three-dimensional incident gusts has been used as equivalent dipole sources in the usual sense of the acoustic analogy in an annular duct. The model has been compared both with rectilinear cascade models and three-dimensional lifting surface models and Euler linearized codes for a benchmark test of the Third computational aeroacoustic workshop. In all cases, the approach is accurate for high hub-to-tip ratio. For a small hub-to-tip ratio, the model deviates from three-dimensional computations, both regarding the blade loading and the acoustic radiation. The radial amplitude variations of the unsteady blade loading are over-estimated and the rectilinear-cascade model exhibits too many radial nodes. As a result, the modal distribution of the radiated acoustic energy is not well-predicted. The main causes of discrepancies are features ignored in the model, such as the modal scattering in radial wave number and the boundary conditions at the end walls. A correction has been proposed to introduce some three-dimensional effects in the original rectilinear-cascade response model, more precisely to introduce the actual annular effect on the wave equation. Then the overall unsteady loading amplitude decreases and the number of radial nodes is reduced. Consequently, the modal distribution is significantly improved, notably with a reduction of the overestimated modes by about 20 percent downstream and 35 percent upstream. However, the differences with full three-dimensional computations are still large, which can be traced to the discrepancies in the unsteady blade loading, particularly near the wall. The results suggest that the proposed correction is necessary to get closer to the underlying physics of the annular-space wave equation, but that it is yet not sufficient to produce acceptable three-dimensional results in this harmonic rather low frequency test case. The development of corrections that could be simply introduced in the rectilinear-cascade model remains a topic of real interest for high-speed broadband-noise computational procedures. For instance, the duct-wall effects could be introduced. The strip-theory approach has finally been applied to predict the wake-interaction broadband noise of the 22-in source diagnostic test (SDT) fan rig of the NASA Glenn Research Center. The strip-theory model resorting to the original rectilinear cascade formulation correctly predicts the shape of the spectrum and the central frequency of the broadband hump. Yet upstream, the levels in the hump are overpredicted by 1–3 dB. The introduction of the correction of the unsteady blade loading formulation reduces the overprediction of the hump, producing consistent prediction in this realistic turbomachinery configuration involving the rotor–stator interaction-noise mechanism. Further improvements of the model could be studied both by investigating new corrections and by introducing the main swirling mean flow effect. The development of corrections that could be simply introduced in the rectilinear-cascade model remains a topic of real interest for high-speed broadband-noise computational procedures.

Acknowledgments

The authors wish to acknowledge Snecma which supported the CIFRE PhD thesis during which this study was conducted. They also would like to acknowledge GAUS, the acoustic groups of l'Université de Sherbrooke (QC, Canada) for supporting the continuation of this work.

References

[1] D.B. Hanson, Theory of broadband noise for rotor and stator cascade with inhomogeneous inflow turbulence including effects of lean and sweep, Contractor Report CR-210762, NASA, 2001.
[2] J.H. Dittmar, J.N. Scott, B.R. Leonard, E.G. Stakolich, Effects of long-chord acoustically treated stator vanes on fan noise. I—Effect of long chord (tapped stator), Technical Note TN-D-8062, NASA, October 1975.
[3] J.H. Dittmar, J.N. Scott, B.R. Leonard, E.G. Stakolich, Effects of long-chord acoustically treated stator vanes on fan noise. II—Effect of acoustical treatment, Technical Note TN-D-8250, NASA, October 1976.
[4] W.N. Dalton, D.B. Elliott, K.L. Nickols, Design of a low speed fan stage for noise suppression, Contractor Report CR-1999-208682, NASA, 1999.
[5] L.J. Heidelberg, Fan noise source diagnostic test—Tone modal structure results, Technical Memorandum TM-2002-211594, NASA, May 2002.
[6] D.L. Sutliff, D.L. Tweedt, E.B. Fite, E. Envia, Low-speed fan noise reduction with trailing edge blowing, Technical Memorandum TM-2002-211559, NASA, June 2002.
[7] J.H. Dittmar, D.M. Elliott, B. Fite, The noise of a forward swept fan, Technical Memorandum TM-2003-212208, NASA, November 2003.
[8] J.J. Berton, M.D. Guynn, Ultrahigh-Bypass-Ratio propulsion systems studied, Technical Memorandum TM-2008-215054, NASA, 2008.
[9] D. Crichton, X. Liping, C.A. Hall, Preliminary fan design for a silent aircraft, *J. Turbomach.* 129 (1) (2007) 184–192.
[10] C.L. Bewick, M.J. Adams, P.J.G. Shwaller, L. Xu, Noise and aerodynamic design and test of a low tip speed fan, *7th AIAA/CEAS Aeroacoustics Conference and Exhibit*, Maastricht, Netherlands, no. AIAA Paper 2001-2268, 2001.
[11] I. Evers, N. Peake, On sound generation by the interaction between turbulence and a cascade of airfoils with non-uniform mean flow, *J. Fluid Mech.* 463 (2002) 25–52.
[12] C.J. Heaton, N. Peake, Algebraic and exponential instability of inviscid swirling flow, *J. Fluid Mech.* 565 (2006) 279–318.
[13] S. Kaji, T. Okazaki, Propagation of sound waves through a blade row, II. Analysis based on the acceleration potential method, *J. Sound Vib.* 11 (3) (1970) 355–375.
[14] S. Kaji, T. Okazaki, Generation of sound by rotor–stator interaction, *J. Sound Vib.* 13 (1970) 281–307.
[15] D.S. Whitehead, Vibration and sound generation in a cascade of flat plates in subsonic flow, Technical Report No.CUED/A-Turbo/TR 15, Cambridge University Engineering Laboratory Report, 1972.
[16] D.S. Whitehead, Classical two-dimensional methods, *AGARD Manual on Aeroelasticity in Axial Flow Turbomachines 1, Unsteady Turbomachinery Aerodynamics* (*AGARD-AG-298*), 1987, pp. 1–30 (Chapter 3).
[17] S.N. Smith, Discrete frequency sound generation in axial flow turbomachines, *Brit. Aeronaut. Res. Coun. R & M* 3709 (1973) 1–59.
[18] M.E. Goldstein, *Aeroacoustics*, McGraw-Hill, New York, 1976.
[19] R. Mani, G. Horvay, Sound transmission through blade rows, *J. Sound Vib.* 12 (1) (1970) 59–83.
[20] W. Koch, On transmission of sound through a blade row, *J. Sound Vib.* 18 (1) (1971) 111–128.
[21] N. Peake, The interaction between a high-frequency gust and a blade row, *J. Fluid Mech.* 241 (1992) 261–289.
[22] N. Peake, The scattering of vorticity waves by an infinite cascade of flat plates in subsonic flow, *Wave Motion* 18 (1993) 255–271.
[23] N. Peake, E.J. Kerschen, A uniform asymptotic approximation of high-frequency unsteady cascade flow, *Proc. R. Soc. London* 449 (1995) 177–186.
[24] S.J. Majumdar, N. Peake, Three-dimensional effects in cascade-gust interaction, *Wave Motion* 23 (1996) 321–337.
[25] S.A.L. Glegg, The response of a swept blade row to a three-dimensional gust, *J. Sound Vib.* 227 (1) (1999) 29–64.
[26] H. Posson, M. Roger, Parametric study of gust scattering and sound transmission through a blade row, *13th AIAA/CEAS Aeroacoustics Conference and Exhibit*, Rome, Italy, no. AIAA Paper 2007-3690, 2007, pp. 1–22.
[27] M. Namba, Three-dimensional flows, *Unsteady Turbomachinery Aerodynamics*, AGARD Manual of Aeroelasticity in Axial Flow Turbomachinery, Vol. AGARD-AG-298, Neuilly sur Seine, France, 1987 (Chapter 7).
[28] H. Kodama, M. Namba, Unsteady lifting surface theory for a rotating cascade of swept blades, *J. Turbomachinery* 112 (1990) 411–417.
[29] J.B.H.M. Schulten, Sound generated by rotor wakes interacting with a leaned vane stator, *AIAA J.* 20-10 (1982) 1352–1358.
[30] J.B.H.M. Schulten, Vane sweep effects on rotor/stator interaction noise, *AIAA J.* 35 (1997) 945–951.
[31] R. Mani, Noise due to interaction of inlet turbulence with isolated stators and rotors, *J. Sound Vib.* 17 (2) (1971) 251–260.
[32] G.F. Homicz, A.R. George, Broadband and discrete frequency radiation from subsonic rotors, *J. Sound Vib.* 36 (1974) 151–177.
[33] R.K. Amiet, Acoustic radiation from an airfoil in a turbulent stream, *J. Sound Vib.* 41 (1975) 407–420.
[34] R.K. Amiet, Noise produced by turbulent flow into propeller or helicopter rotor, *AIAA J.* 15 (1977) 307–308 (also AIAA Paper 76–560).
[35] M. Roger, S. Moreau, A. Guedel, Broadband fan noise prediction using single-airfoil theory, Noise Control Eng. J. 54(1) (2006) 5–14.
[36] S. Moreau, M. Roger, Competing broadband noise mechanisms in low-speed axial fans, *AIAA J.* 45 (1) (2007) 48–57.
[37] S.A.L. Glegg, Broadband noise from ducted prop fans, *15th Aeroacoustics Conference*, Long Beach, CA, no. AIAA Paper 1993-4402, 1993, pp. 1–14.
[38] B. De Gouville, M. Roger, J.M. Cailleau, Prediction of fan broadband noise, *4th AIAA/CEAS Aeroacoustics Conference and Exhibit*, Toulouse, France, no. AIAA Paper 98-2317, 1998.
[39] P. Joseph, A. Parry, Rotor/wall boundary-layer interaction broadband noise in turbofan engines, *7th AIAA/CEAS Aeroacoustics Conference and Exhibit*, Maastricht, Netherlands, no. AIAA Paper 2001-2244, 2001, pp. 1–11.
[40] C.S. Ventres, M.A. Theobald, W.D. Mark, Turbofan noise generation, volume 1: analysis, Contractor Report CR-167952, NASA, 1982.
[41] M. Nallasamy, E. Envia, Computation of rotor wake turbulence noise, *J. Sound Vib.* 282 (2005) 649–678.
[42] A. Ravindranath, B. Lakshminarayana, Three dimensional mean flow and turbulence characteristics of the near wake of the compressor rotor blade, Contractor Report 159518 PSU Turbo R 80-4, NASA, 1980.
[43] U.W. Ganz, P.D. Joppa, T.J. Patten, D.F. Scharpf, Boeing 18-inch fan rig broadband noise test, Contractor Report CR-1998-208704, NASA, 1998.
[44] D.B. Hanson, The spectrum of rotor noise caused by atmospheric turbulence, *J. Acoust. Soc. Am.* 56 (1) (1974) 110–126.
[45] S.A.L. Glegg, N. Walker, Fan noise from blades moving through boundary layer turbulence, *5th AIAA/CEAS Aeroacoustics Conference and Exhibit*, Bellevue, WA, no. AIAA Paper 1999-1888, 1999.
[46] D.B. Hanson, K.P. Horan, Turbulence/cascade interaction: spectra of inflow, cascade response, and noise, *4th AIAA/CEAS Aeroacoustics Conference and Exhibit*, Toulouse, France, no. AIAA Paper 1998-2319, 1998, pp. 688–700.
[47] J.C. Hardin, D. Huff, C.K. Tam, Benchmark problems, in: N.G.R. C. Dahl, (Eds.), *Third Computational Aeroacoustics (CAA) Workshop on Benchmark Problems*, no. NASA Conference Publication 2000-209790, 2000, pp. 1–22.
[48] C.E. Hughes, Aerodynamic performance of scale-model turbofan outlet guide vanes designed for low-noise, *8th AIAA/CEAS Aeroacoustics Conference and Exhibit*, Breckenridge, Colorado, no. AIAA Paper 2002-0374/NASA/TM-2001-211352, 2002.
[49] C.E. Hughes, R.J. Jeracki, R.P. Woodward, C.J. Miller, Fan noise source diagnostic test—rotor alone aerodynamic performance results, *8th AIAA/CEAS Aeroacoustics Conference and Exhibit*, Breckenridge, Colorado, no. AIAA Paper 2002-2426, 2002.

[50] G.G. Podboy, M.J. Krupar, C.E. Hughes, R.P. Woodward, Fan noise source diagnostic test—LDV measured flow field results, *8th AIAA/CEAS Aeroacoustics Conference and Exhibit*, Breckenridge, Colorado, no. AIAA Paper 2002-2431/NASA/TM-2003-212330, 2002.
[51] R.P. Woodward, C.E. Hughes, R.J. Jeracki, C.J. Miller, Fan noise source diagnostic test—far-field acoustic results, Technical Memorandum TM-2002-211591, NASA, May 2002.
[52] S.A.L. Glegg, Broadband fan noise generated by small scale turbulence, Contractor Report CR-207752, NASA, 1998.
[53] R. Raj, B. Lakshminarayana, Three dimensional characteristics of turbulent wakes behind rotors of axial flow turbomachinery, *J. Eng. Power* 98 (1976) 218–228.
[54] B. Elhadidi, H.M. Atassi, Sound generation and scattering from radial vanes in uniform flow, *Proceedings of ICFDP7, Seventh International Conference of Fluid Dynamics and Propulsion*, 19–21 December, Sharm El-Sheikh, Egypt AAC-3, 2001, pp. 1–11.
[55] M. Namba, J.B.H.M. Schulten, Category 4—fan stator with harmonic excitation by rotor wake, in: J. Hardin, D. Huff, C. Tam (Eds.), *Third Computational Aeroacoustics (CAA) Workshop on Benchmark Problems*, no. NASA Conference Publication 2000-209790, 2000, pp. 73–86.
[56] A.A. Ali, H.M. Atassi, Scattering of acoustic and vorticity disturbances by an unloaded annular cascade in a swirling flow, *8th AIAA/CEAS Aeroacoustics Conference and Exhibit*, no. AIAA Paper 2002-2559, 2002, pp. 1–11.
[57] O.V. Atassi, A.A. Ali, Inflow/outflow conditions for time-harmonic internal flows, *J. Comput. Acoust.* 10 (2) (2002) 152–182.
[58] D. Prasad, J.M. Verdon, A three-dimensional linearized Euler analysis of classical wake/stator interactions: validation and unsteady response predictions, *Aeroacoustics* 1 (2) (2002) 137–163.
[59] J.B.H.M. Schulten, Sound Generation by Ducted Fans and Propellers as a Lifting Surface Problem, PhD Thesis, University of Twente, 1993.
[60] H.M. Atassi, A.A. Ali, O.V. Atassi, I.V. Vinogradov, Scattering of incidence disturbances by an annular cascade in a swirling flow, *J. Fluid Mech.* 499 (2004) 111–138.
[61] M.D. Montgomery, J.M. Verdon, A 3D linearized unsteady Euler analysis for turbomachinery blade rows, part 1: aerodynamic and numerical formulations, part 2: unsteady aerodynamic response predictions, in: T.H. Fransson (Ed.), *Unsteady Aerodynamics and Aeroelasticity of Turbomachines*, Kluwer, Dordrecht, Netherlands, 1998, pp. 427–464.
[62] J.M. Verdon, Linearized unsteady aerodynamic analysis of the acoustic response to wake/blade-row interaction, Contractor Report CR-2001-210713, NASA, 2001.
[63] M.E. Goldstein, *Aeroacoustics*, McGraw-Hill, New York, 1976, pp. 219–248 (Chapter 5).
[64] H.M. Atassi, G. Hamad, Sound generated in a cascade by three-dimensional disturbances convected in subsonic flow, *7th AIAA Aeroacoustics Conference*, Palo Alto, California, no. AIAA Paper 1981-2046, 1981, pp. 1–13.
[65] D.P. Lockard, An efficient, two-dimensional implementation of the Ffowcs Williams and Hawkings equation, *J. Sound Vib.* 229 (4) (2000) 897–911.
[66] J.M. Tyler, T.G. Sofrin, Axial flow field of an axial compressor noise studies, SAET 70 (1962) 309–332.
[67] H. Posson, M. Roger, Experimental validation of a cascade response function for fan broadband noise predictions, *14th AIAA/CEAS Aeroacoustics Conference and Exhibit*, Vancouver, Canada, no. AIAA Paper 2008-2844, 2008, pp. 1–20.
[68] E. Envia, D.L. Tweedt, R.P. Woodward, D.M. Elliott, E.B. Fite, C.E. Hughes, G.G. Podboy, D.L. Sutliff, An assessment of current fan noise prediction capability, *14th AIAA/CEAS Aeroacoustics Conference and Exhibit*, Vancouver, Canada, no. AIAA Paper 2008-2991, 2008, pp. 1–46.
[69] H. Posson, S. Moreau, M. Roger, Fan-OGV broadband noise prediction using a cascade response, *15th AIAA/CEAS Aeroacoustics Conference and Exhibit*, Vancouver, Canada, no. AIAA Paper 2009-3150, 2009, pp. 1–18.